

Redescription of *Monacha pantanellii* (De Stefani, 1879), a species endemic to the central Apennines, Italy (Gastropoda, Eupulmonata, Hygromiidae) by an integrative molecular and morphological approach

Joanna R. Pieńkowska¹, Giuseppe Manganelli², Folco Giusti², Debora Barbato²,
Ewa Kosicka¹, Alessandro Hallgass², Andrzej Lesicki¹

1 Department of Cell Biology, Institute of Experimental Biology, Faculty of Biology, Adam Mickiewicz University in Poznan, Uniwersytetu Poznańskiego 6, 61-614 Poznań, Poland **2** Dipartimento di Scienze Fisiche, della Terra e dell'Ambiente, Università di Siena, Via Mattioli 4, 53100 Siena, Italy

Corresponding author: Andrzej Lesicki (alesicki@amu.edu.pl)

Academic editor: E. Neubert | Received 11 July 2020 | Accepted 25 September 2020 | Published 6 November 2020

<http://zoobank.org/6806D201-2ABF-4A8C-B06C-A7A31CDF852D>

Citation: Pieńkowska JR, Manganelli G, Giusti F, Barbato D, Kosicka E, Hallgass A, Lesicki A (2020) Redescription of *Monacha pantanellii* (De Stefani, 1879), a species endemic to the central Apennines, Italy (Gastropoda, Eupulmonata, Hygromiidae) by an integrative molecular and morphological approach. ZooKeys 988: 17–61. <https://doi.org/10.3897/zookeys.988.56397>

Abstract

Specimens obtained from ten populations of a *Monacha* species from the central Apennines were compared with six molecular lineages of *Monacha cantiana* s. l. (CAN-1, CAN-2, CAN-3, CAN-4, CAN-5, CAN-6) and two other *Monacha* species (*M. cartusiana* and *M. parumincta*), treated as outgroup, by molecular (nucleotide sequences of two mitochondrial COI and 16S rDNA as well as two nuclear ITS2 and H3 gene fragments) and morphological (shell and genital anatomy) analysis. The results strongly suggest that these populations represent a separate species for which two names are available: the older *Helix pantanellii* De Stefani, 1879 and the junior *M. ruffoi* Giusti, 1973. The nucleotide sequences created well separated clades on each phylogenetic tree. Genital anatomy included several distinctive features concerning vaginal appendix, penis, penial papilla and flagellum; instead, shell characters only enabled them to be distinguished from *M. cartusiana* and *M. parumincta*. Remarkably, populations of *M. pantanellii* show high morphological variability. Shell variability mainly concerns size, some populations having very small

dimensions. Genital variability shows a more intricate pattern of all anatomical parts, being higher as regards the vagina and vaginal appendix. Despite this morphological variability, the K2P distance range of COI sequences between populations is narrow (0.2–4.5%), if we consider all but three of the 53 sequences obtained. This research confirmed that the species of *Monacha* and their molecularly distinguished lineages can only occasionally be recognised morphologically and that they have significant inter- and intra-population variability. The possibility of using an overall approach, including shell, genital and molecular evidence, was taken in order to establish a reliable taxonomic setting.

Keywords

16S rDNA, COI, H3, ITS2, molecular features, shell and genital structure, species distribution

Introduction

Land snail fauna of the central and southern Apennines of Italy includes many common, widespread and diversified helicoideans, such as the geometrids *Candidula* Kobelt, 1871 and *Xerogyra* Monterosato, 1892, the hygromiid *Monacha* Fitzinger, 1833, the helicids *Marmorana* Hartmann, 1844 and *Helix* Linnaeus, 1758. Despite this, their taxonomy, systematics and phylogenetics have been challenging since the early studies exclusively based on shell features. Taxonomic revisions of the second half of the 20th century (e.g., Forcart 1965; Giusti 1973) lumped many of the earliest described taxa on the basis of a similar gross genital morphology. However, more recent investigations using protein electrophoresis/allozymes (*Marmorana*: Oliverio et al. 1993) and mitochondrial and nuclear gene sequences (*Marmorana*: Fiorentino et al. 2010; *Helix*: Fiorentino et al. 2016) shed new light on these variable species and radiation may explain the relationship between the lineages or clades distinguished in the Apennines.

Continuing work on the hygromiid *Monacha* (Pieńkowska et al. 2015, 2016, 2018a, 2018b, 2019a, 2019b), we studied species living in the mountain grasslands of the central Apennines, whence came reports of three species, the widespread *M. cantiana* (Montagu, 1803) and the endemic *M. orsini* (Villa and Villa, 1841) and *M. ruffoi* Giusti, 1973, and a number of taxa with uncertain taxonomic status (Alzona 1971; Manganelli et al. 1995). We conducted a joint molecular and morphological study of many populations, finding many different species or their molecular lineages. However, it was difficult to draw reliable nomenclatural and taxonomic conclusions because the identity of the earliest taxa, established in the past, were often based on non-diagnostic shell characters of specimens without any precise collecting record.

A first result of our research corroborated the specific distinctness of *Monacha ruffoi* Giusti, 1973, of which we discovered an overlooked senior synonym: *Helix pantanellii* De Stefani, 1879.

The aim of the present research was: 1) to investigate phylogenetic relationships of *Monacha pantanellii* with other *Monacha* species or their molecular lineages; 2) to evaluate its morphological variability; 3) to redescribe the species.

Materials and methods

Taxonomic sampling

Ten populations of *Monacha pantanellii* (Table 1, Fig. 1) were considered in our analysis of their molecular and morphological (shell and genitalia structure) variability, and compared with the *M. cantiana* s. l. lineages (Pieńkowska et al. 2018a, 2019b). The sequences deposited in GenBank were also considered for the molecular analysis (Table 2). Two other *Monacha* species were used for morphological and molecular comparison: *M. cartusiana* (Müller, 1774) and *M. parumcincta* (Rossmässler, 1834). Another 23 populations of *M. pantanellii* were studied on a qualitative morphological basis (they were not included in the statistical analysis) (Table 3).

Material examined

New material examined is listed as follows, when possible: geographic coordinates (Lat & Long and UTM references) of locality, locality (country, region, site, municipality and province), collector(s), date, number of specimens (sh/s shell/shells; spcm/spcms specimen/specimens), and collection where material is kept in parenthesis (Tables 1, 3). The material is kept in the F. Giusti collection (**FGC**; Dipartimento di Scienze Fisiche, della Terra e dell'Ambiente, Università di Siena, Italy). The material used for comparison has already been described (see Pieńkowska et al. 2018a: table 1, 2019b: table 1).

Molecular study

Fifty-eight specimens representing ten population of *Monacha pantanellii* were used for molecular analysis (Table 1). DNA extraction, amplification and sequencing methods are described in detail in our previous paper (Pieńkowska et al. 2018a).

Two mitochondrial and two nuclear gene fragments were analysed, namely cytochrome c oxidase subunit 1 (COI), 16S ribosomal DNA (16S rDNA), an internal transcribed spacer of rDNA (ITS2) and histone 3 (H3), respectively. All new sequences were deposited in GenBank (Table 1). The COI, 16S rDNA, ITS2 and H3 sequences obtained from GenBank for comparison are listed in Table 2.

The sequences were edited by eye using the programme BioEdit, version 7.2.6 (Hall 1999, BioEdit 2017). Alignments were performed using CLUSTALW (Thompson et al. 1994) implemented in MEGA7 (Kumar et al. 2016). The COI and H3 sequences were aligned according to the translated amino acid sequences. The ends of all sequences were trimmed. The lengths of the sequences after trimming were 592 bp for COI, 286 positions for 16S rDNA, 501 positions for ITS2 and 279 bp for H3. The sequences were collapsed to haplotypes (COI and 16S rDNA) and to common sequences (ITS2 and H3) using the programme ALTER (Alignment Transformation EnviRonment) (Glez-Peña et al. 2010). Gaps and ambiguous positions were removed from alignments prior to phylogenetic analysis. Mitochondrial (COI and 16S rDNA) and nuclear (ITS2

No.	Coordinates (Lat & Long / UTM references)	Localities Country and site	Collector / date / no. of specimens (collection)	Clade	Popu- lation	COI		16S rDNA		ITS2		H3		Figs
						New haplotype (no. spcms.)	GenBank ##	New haplotype (no. spcms.)	GenBank ##	New common sequence (no. spcms)	GenBank ##	New common sequence (no. spcms)	GenBank ##	
6	42°15.38'N, 12°50.32'E 33TUG28	Italy, Latium, Via Salaria, 650 m NW of Poggio San Lorenzo (Poggio San Lorenzo, Rieti), 400 m a.s.l.	A. Hallgass / 10.2013 / 6 (FGC 41551)	PAN	Lor	COI 19 (1) COI 20 (1) COI 21 (4)	MT380032 MT380033 MT380034	16S 8 (2) 16S 10 (4)	MT376056 MT376057 MT376058	ITS2 9 (1) ITS2 5 (2) ITS2 9 (1)	MT376104 MT376105 MT376106	H3 6 (1) H3 9 (1) H3 1 (1)	MT385802 MT385803 MT385804	23-25
	7	42°12.81'N, 12°57.80'E 33TUG37	Italy, Latium, near the bridge on Lago del Turano (Castel di Torà, Rieti), 260 m a.s.l.	PAN	Tur2	COI 22 (1) COI 23 (1) COI 24 (3)	MT380038 MT380039 MT380040	16S 12 (2) 16S 13 (3)	MT376062 MT376063 MT376064	ITS2 10 (1) ITS2 2 (2) ITS2 2 (2)	MT376110 MT376111 MT376112	H3 13 (1) H3 14 (1) H3 1 (2)	MT385809 MT385808 MT385810	15-17, 57-59
						COI 25 (1) COI 26 (1) COI 27 (3)	MT380042 MT380043 MT380044	16S 14 (1) 16S 15 (1) 16S 16 (3)	MT376066 MT376067 MT376068	ITS2 5 (1) ITS2 11 (1) ITS2 5 (1)	MT376113 MT376114 MT376115	H3 9 (2) H3 1 (1) H3 10 (1)	MT385811 MT385812 MT385813	
8	42°07.88'N, 13°01.67'E 33TUG36	Italy, Latium, Valle del Turano, 1,6 km ESE di Turania (Turania, Rieti), 570 m a.s.l.	A. Hallgass / 04.11.2013 / 7 (FGC 42971)	PAN	Tur1	COI 28 (1) COI 29 (1) COI 22 (1) COI 30 (1)	MT380046 MT380047 MT380050 MT380051	16S 17 (1) 16S 18 (1) 16S 12 (1) 16S 19 (1)	MT376070 MT376071 MT376072 MT376074	ITS2 12 (1) ITS2 11 (1) ITS2 11 (3) ITS2 5 (1)	MT376116 MT376117 MT376118 MT376119 MT376120	H3 9 (2) H3 9 (2) H3 1 (3) MT385819 MT385820 MT385821	11-14, 62	
	9	42°05.74'N, 13°03.56'E 33TUG36	Italy, Abruzzi, Carsoli, industrial area (Carsoli, L'Aquila), 600 m a.s.l.	PAN	Car	COI 19 (1) COI 31 (1) COI 32 (1)	MT380052 MT380053 MT380054	16S 8 (1) 16S 20 (1) 16S 21 (1)	MT376076 MT376077 MT376078	ITS2 11 (1) ITS2 11 (1) ITS2 5 (2)	MT376121 MT376122 MT376123	H3 9 (4) H3 9 (4) H3 9 (1)	MT385822 MT385823 MT385824	30-31, 53-56
						COI 8 (2) COI 33 (2) COI 34 (1) COI 35 (1) COI 36 (3)	MT380056 MT380057 MT380058 MT380060 MT380061	16S 19 (1) 16S 23 (2) 16S 16 (1) 16S 24 (1) 16S 25 (3)	MT376080 MT376081 MT376082 MT376083 MT376085	ITS2 7 (1) ITS2 5 (2) ITS2 13 (1) ITS2 14 (1) ITS2 15 (1)	MT376124 MT376125 MT376126 MT376127 MT376128	H3 6 (1) H3 9 (1) H3 1 (1) H3 15 (1) H3 9 (1)	MT385825 MT385826 MT385827 MT385828 MT385829	
10	42°02.85'N, 12°54.33'E 33TUG25	Italy, Latium, Valle dell'Aniene, 600 m ESE of Rocciogiovine (Rocciogiovine, Rome), 380 m a.s.l.	A. Hallgass / 10.2013 / 7 (FGC 42974)	PAN	Ani	COI 32 (1) COI 35 (1) COI 36 (3)	MT380055 MT380056 MT380057	16S 22 (1) 16S 22 (1) 16S 23 (2)	MT376079 MT376080 MT376081	ITS2 5 (2) ITS2 5 (2) ITS2 5 (2)	MT376123 MT376124 MT376125	H3 9 (1) H3 9 (1) H3 9 (1)	MT385824 MT385825 MT385826	26-29, 49-52, 60

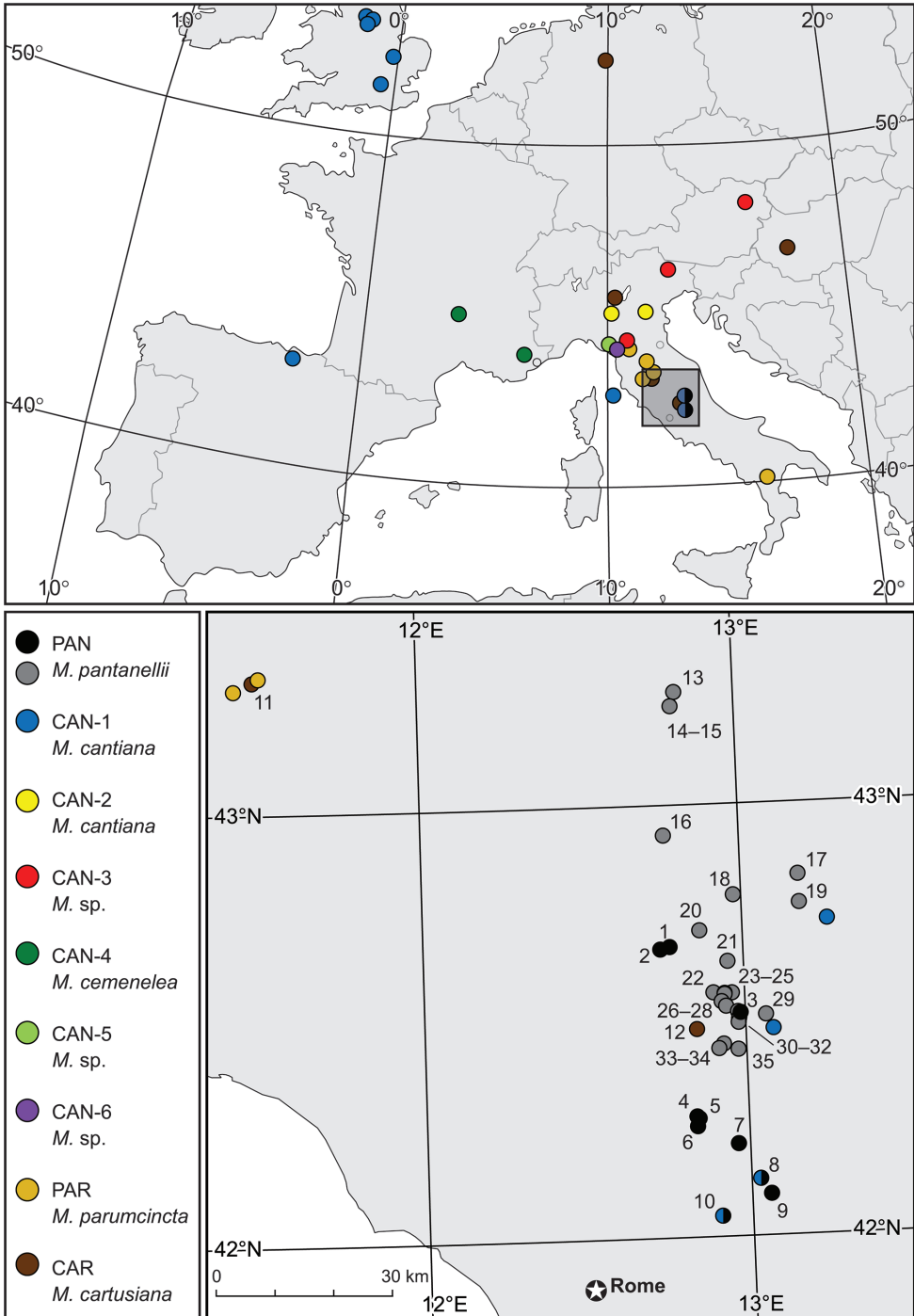


Figure 1. Localities of *Monacha pantanellii* and *M. cartusiana* populations listed in Tables 1, 3 (*M. pantanellii* black circles Table 1, grey circles Table 3). Details of localities of other *Monacha* species and their molecular lineages were provided in previous papers (Pieńkowska et al. 2015, 2018a, 2018b, 2019b).

Table 2. GenBank sequences used for molecular analysis comparisons.

Species	COI	16S rDNA	ITS2	H3	References
CAN-1 (<i>Monacha cantiana</i> s. s.)	MG208884–	MG208960–	MH137963–	MG209031–	Pierikowska et al. (2018a)
	MG208924	MG208995	MH137978	MG209039	
	–	–	–	MG209041–	Pierikowska et al. (2018a)
CAN-2 (<i>Monacha cantiana</i> s. s.)	MG208925–	MG208996–	MH137979–	MG209048	
	MG208932	MG209004	MH137981	MG209049–	Pierikowska et al. (2018a)
	–	–	MK067000	MG209052	
CAN-3 (<i>Monacha</i> sp.)	MG208933–	MG209005–	MH137982–	MG209040	Pierikowska et al. (2019b)
	MG208938	MG209010	MH137983	MG209040	Pierikowska et al. (2018a)
	–	–	–	MG209053–	Pierikowska et al. (2018a)
CAN-4 (<i>Monacha cemelelea</i>)	–	–	MK067001–	MG209057	
	–	–	MK067002	–	Pierikowska et al. (2019b)
	MG208939–	MG209011–	MH137984	MG209058–	Pierikowska et al. (2018a)
CAN-5 (<i>Monacha</i> sp.)	MG208943	MG209015	–	MG209060	
	–	–	MK067003–	–	Pierikowska et al. (2019b)
	–	–	MK067004	–	
CAN-6 (<i>Monacha</i> sp.)	MK066929–	MK066947–	MK066981–	MK066965–	Pierikowska et al. (2019b)
	MK066941	MK066959	MK066994	MK066977	
PAR (<i>Monacha parumcincta</i>)	MK066942–	MK066960–	MK066995–	MK066978–	Pierikowska et al. (2019b)
	MK066946	MK066964	MK066999	MK066980	
CAR (<i>Monacha cartusiana</i>)	MG208944–	MG209016–	MH137985–	MG209061–	Pierikowska et al. (2018a)
	MG208959	MG209030	MH137992	MG209071	
	–	–	MK067005	–	Pierikowska et al. (2019b)
CAR (<i>Monacha cartusiana</i>)	KM247376	KM247391	–	–	Pierikowska et al. (2015)
	–	–	MH137993	MG209072	Pierikowska et al. (2018a)
	MH203998	MH204081	–	–	Pierikowska et al. (2018b)

and H3) sequences were concatenated (Table 4) before phylogenetic analysis. Finally, the sequences of COI, 16S rDNA, ITS2 and H3 were concatenated (Table 4) for Maximum Likelihood (ML) and Bayesian Inference (BI).

Estimates of evolutionary divergence between the sequences of COI obtained in this study and other sequences from GenBank were conducted with MEGA7 using the Kimura two-parameter model (K2P) (Kimura 1980). The analysis involved 83 nucleotide sequences. All positions containing gaps and missing data were eliminated. There was a total of 615 positions in the final dataset.

Maximum Likelihood (ML) analyses were then performed with MEGA7. *Monacha cartusiana* and *Monacha parumcincta* were added as outgroup species in each analysis. For ML analysis of concatenated sequences, the following best nucleotide substitution models were specified according to the Bayesian Information Criterion (BIC): HKY+G+I (Hasegawa et al. 1985, Kumar et al. 2016) for COI and 16S rDNA concatenated sequences of 878 positions (592 COI + 286 16S rDNA), T92+G+I (Tamura 1992, Kumar et al. 2016) for ITS2+H3 concatenated sequences of 780 positions (501 ITS2 + 279 H3), and T92+G+I for COI+16S rDNA+ITS2+H3 concatenated sequences with a total length of 1658 positions (592 COI + 286 16S rDNA + 501 ITS2 + 279 H3). Bayesian analysis was conducted with MRBAYES 3.1.2 (Ronquist and Huelsenbeck 2003) using the evolution model already used for ML calculation. Four Monte Carlo Markov chains were run for one million generations, sampling every 100 generations (the first 250,000 trees were discarded as ‘burn-in’). This gave us

Table 3. Populations and materials of *Monacha cartusiana* (CAR) and *Monacha pantanellii* (PAN) not listed in Table 1 because they were not included in the molecular and statistical morphological analysis (apart from additional morphological analysis of *M. cartusiana*). A question mark before the geographical coordinates of some localities denotes that the georeferencing was done a posteriori on the basis of the available information.

No.	Species	Coordinates (Lat & Long / UTM references)	Country and site (municipality and province in parenthesis)	Collector / Date / No. of specimens (collection)	Remarks
11	CAR	43°18.45'N, 11°28.88'E 32TQN09	Italy, Tuscany, Stazione di Castelnuovo Berardenga (Asciano, Siena)	G. Manganelli / 01.11.1981 / spcm (FGC 3430)	–
12	CAR	? 42°28.85'N, 12°50.84'E 33TUH20	Italy, Latium, Lago Lungo (Rieti, Rieti)	F. Giusti / 14.08.1966 / spcm (FGC 23875)	–
13	PAN	? 43°15.67'N, 12°48.83'E 33TUH29	Italy, Umbria, Val Sorda (Gualdo Tadino, Perugia), 1,050 m a.s.l.	A. Minelli / 03.08.1969 / 6 spcms (FGC 25350)	–
14	PAN	? 43°13.72'N, 12°48.02'E 33TUH28	Italy, Umbria, Gualdo Tadino (Gualdo Tadino, Perugia)	F. Giusti / 26.10.1967 / 4 shs (FGC636); 2 spcms (FGC 25352)	–
15	PAN	43°13.72'N, 12°48.02'E 33TUH28	Italy, Umbria, La Rocchetta (Gualdo Tadino, Perugia)	F. Giusti & G. Manganelli / 13.12.1984 / 1 spcm (FGC 6371) / L. Favilli & G. Manganelli / 01.10.1992 / 4 spcms (FGC 6370)	–
16	PAN	42°55.83'N, 12°45.83'E 33TUH15	Italy, Umbria, 600 m a E di Roviglietto (Foligno, Perugia), 510 m a.s.l.	A. Hallgass / 25.09.2010 /	–
17	PAN	42°49.92'N, 13°10.87'E 33TUH54	Italy, Umbria, Monti Sibillini, Valle Canatra (Norcia, Perugia)	F. Giusti & G. Manganelli / 13.09.1988 / 6 shs and 3 spcms (FG 25360)	–
18	PAN	42°47.33'N, 12°58.55'E 33TUH33	Italy, Umbria, Gole di Biselli (Norcia, Perugia)	A. Hallgass / 07.10.2011 /	–
19	PAN	42°46.00'N, 13°10.90'E 33TUH53	Italy, Umbria, Monti Sibillini, Costa Precino (Norcia, Perugia), 1,500 m a.s.l.	A. Benocci, M. Bianchi & G. Manganelli / 29.06.2014 / 2 spcms (FGC 42293)	–
20	PAN	42°42.52'N, 12°51.98'E 33TUH23	Italy, Umbria, 750 m E of Caso (Sant'Anatolia di Narco, Perugia), 800 m a.s.l.	A. Hallgass / 18.09.2010 /	–
21	PAN	42°38.14'N, 12°57.04'E 33TUH32	Italy, Umbria, 1 km SSW of Ruscio (Monteleone di Spoleto, Perugia)	A. Vannozi / 22.08.2010 /	–
22	PAN	42°33.85'N, 12°54.17'E 3TUH21	Italy, Latium, Monti Reatini, Strada regionale 521 di Morro (Leonessa, Rieti), 1,050 m a.s.l.	A. Hallgass / 13.09.2009 /	–
23	PAN	? 42°33.75'N, 12°57.63'E 33TUH31	Italy, Latium, Monti Reatini, Leonessa (Leonessa, Rieti), 1,000 m a.s.l.	F. Giusti / 04.08.1966 / 1 sh and 1 spcm (FGC 25348)	Paratypes of <i>Monacha ruffoi</i> Giusti, 1973
24	PAN	? 42°33.72'N, 12°56.27'E 33TUH31	Italy, Latium, Monti Reatini, Monte Tilia (Leonessa, Rieti), 1,600 m a.s.l.	F. Giusti / 06.08.1966 / 11 shs and 3 spcms (FGC 25337)	Material collected by F. Giusti in 1966 in part published (3 spcms) and in part not published (11 shs). Unfortunately the 3 spcms, constituting paratypes of <i>Monacha ruffoi</i> Giusti, 1973, have been lost.
25	PAN	? 42°33.58'N, 12°56.25'E 33TUH31	Italy, Latium, Monti Reatini, Monte Tilia (Leonessa, Rieti), 1,600-1,700 m a.s.l.	F. Giusti / 12.08.1966 / 3 shs (FGC 25338)	Material collected by F. Giusti in 1966 but not published.
26	PAN	? 42°32.58'N, 12°55.65'E 33TUH21	Italy, Latium, Monti Reatini, Monte Corno (Leonessa, Rieti), 1,600 m a.s.l.	F. Giusti / 12.08.1966 / 6 spcms, 2 of which dissected (FGC 25342) / 16 shs (FGC 25340) / 5 shs (FGC 25341)	Paratypes of <i>Monacha ruffoi</i> Giusti, 1973

No.	Species	Coordinates (Lat & Long / UTM references)	Country and site (municipality and province in parenthesis)	Collector / Date / No. of specimens (collection)	Remarks
27	PAN	ϕ 42°31.93'N, 12°56.45'E 33TUH31	Italy, Latium, Monti Reatini, Rio Fuggio (Leonessa, Rieti), 1,300 m a.s.l.	F. Giusti / 05.08.1966 / 5 spcms (FGC 25351)	Paratypes of <i>Monacha ruffoi</i> Giusti, 1973
28	PAN	ϕ 42°31.13'N, 12°58.63'E 33TUH30	Italy, Latium, Monti Reatini, Vallonina (Leonessa, Rieti), 1,100 m a.s.l.	F. Giusti / 03.08.1966 / 1 spcm (FGC 25343) / 12 shs and 21 spcms (FGC 25344) / 21 spcms, 3 of which dissected (FGC 25345)	Holotype (FGC 25343) and paratypes (FGC 25344 and 25345) of <i>Monacha ruffoi</i> Giusti, 1973. Other 5 paratypes from this site have been subject to molecular and morphological study (see Table 1, no. 3)
			Italy, Latium, Monti Reatini, Vallonina (Leonessa, Rieti), 1,100 m a.s.l., along Fiume Corno	F. Giusti / 03.08.1966 / 5 shs (FGC 25347)	Material collected by F. Giusti in 1966 but not published.
29	PAN	ϕ 42°30.63'N, 13°03.85'E 33TUH40	Italy, Latium, Monti Reatini, Monte Cavalli (Posta, Rieti)	F. Giusti / 15.08.1966 / 1 spcm dissected and drawn (FGC)	Material collected by F. Giusti in 1966 but not published and lost.
30	PAN	ϕ 42°30.30'N, 12°58.82'E 33TUH30	Italy, Latium, Monti Reatini, pathway to Monte Sassetelli (Cantalice, Rieti), 1,500 m a.s.l.	F. Giusti / 13.08.1966 / 3 spcms (FGC 25355)	Paratypes of <i>Monacha ruffoi</i> Giusti, 1973
31	PAN	ϕ 42°30.12'N, 12°58.77'E 33TUH30	Italy, Latium, Monti Reatini, pathway to Monte Sassetelli (Cantalice, Rieti), 1,550 m a.s.l.	F. Giusti / 13.08.1966 / 3 spcms (FGC 25354)	Material collected by F. Giusti in 1966 but not published.
32	PAN	ϕ 42°29.63'N, 12°58.67'E 33TUH30	Italy, Latium, Monti Reatini, pathway to Monte Sassetelli (Cantalice, Rieti), 1,550- 1,750 m a.s.l.	F. Giusti / 13.08.1966 / 3 shs (FGC 25349)	Material collected by F. Giusti in 1966 but not published.
33	PAN	ϕ 42°26.70'N, 12°55.77'E 33TUH20	Italy, Latium, Monti Reatini, above Lisciano (Rieti, Rieti), 800 m a.s.l.	F. Giusti / 6.08.1966 / 14 shs and 2 spcms, 1 of which dissected and drawn (FGC 10890)	Paratypes of <i>Monacha ruffoi</i> Giusti, 1973; dissected specimen lost
34	PAN	ϕ 42°26.09'N, 12°54.86'E 33TUH20	Italy, Latium, Monti Reatini, Vazia (Rieti, Rieti), 400 m a.s.l.	F. Giusti / 11.08.1966 / 1 spcm dissected and drawn (FGC)	Material collected by F. Giusti in 1966 but not published and lost.
35	PAN	ϕ 42°25.90'N, 12°58.45'E 33TUG39	Italy, Latium, Monti Reatini, Pian di Stura (Cittaducale, Rieti)	F. Giusti / 07.08.1966 / 1 spcm dissected and drawn (FGC)	Material collected by F. Giusti in 1966 but not published and lost.

a 50% majority rule consensus tree. In parallel, Maximum Likelihood (ML) analysis was performed with MEGA7 (Kumar et al. 2016) and calculated bootstrap values were mapped on the 50% majority rule consensus Bayesian tree.

Morphological study

One hundred and thirty-four specimens representing *M. pantanellii*, *M. cantiana* s. l., *M. parumcincta* and *M. cartusiana* were considered to investigate shell variability between these four species (including six molecular lineages of *M. cantiana* s. l.) (see Table 1 and Pieńkowska et al. 2018a, 2019b); the 43 specimens of nine populations of *M. pantanellii* (Fio1, Val, Sab, Alt, Lor, Tur2, Tur1, Car and Ani, see Table 1) were also considered to investigate shell variability between specimens of these populations. Shell variability was analysed randomly choosing five adult specimens from each population, when possible. Twelve shell variables were measured to the nearest

Table 4. Concatenated sequences of COI+16S rDNA and ITS2+H3 for ML analysis (Figs 2, 3) and COI+16S rDNA+ITS2+H3 for Bayesian analysis (Fig. 4).

Concatenated sequence	COI haplotype	16S rDNA haplotype	Concatenated sequence	COI haplotype	16S rDNA haplotype	ITS2 common sequence	H3 common sequence	Concatenated sequence	COI haplotype	16S rDNA haplotype	ITS2 common sequence	H3 common sequence	Locality / population
<i>Monacha pantanelli</i> PAN													
COI16S 1	COI 33	16S 23	ITS2H3 1	COI 33	16S 23	ITS2 5	H3 6	CS 1	COI 33	16S 23	ITS2 5	H3 6	IT, Latium, Valle dell'Aniene [Ani]
COI16S 2	COI 34	16S 16	ITS2H3 2	COI 34	16S 16	ITS2 5	H3 1	CS 2	COI 34	16S 16	ITS2 5	H3 1	IT, Latium, Valle dell'Aniene
COI16S 3	COI 36	16S 25	ITS2H3 3	COI 36	16S 25	ITS2 14	H3 9	CS 3	COI 36	16S 25	ITS2 14	H3 9	IT, Latium, Valle dell'Aniene
			ITS2H3 4	COI 36	16S 25	ITS2 15	H3 14	CS 4	COI 36	16S 25	ITS2 15	H3 14	IT, Latium, Valle dell'Aniene
			ITS2H3 5	COI 36	16S 25	ITS2 7	H3 9	CS 5	COI 36	16S 25	ITS2 7	H3 9	IT, Latium, Valle dell'Aniene
COI16S 4	COI 35	16S 24	ITS2H3 6	COI 35	16S 24	ITS2 13	H3 15	CS 6	COI 35	16S 24	ITS2 13	H3 15	IT, Latium, Valle dell'Aniene
COI16S 5	COI 9	16S 7											IT, Latium, Omaro Alto, Montenero Sabino [Sab]
COI16S 6	COI 11	16S 8						CS 7	COI 11	16S 8	ITS2 5	H3 1	IT, Latium, Omaro Alto, Montenero Sabino
COI16S 7	COI 12	16S 8	ITS2H3 7	COI 12	16S 8	ITS2 6	H3 10	CS 8	COI 12	16S 8	ITS2 6	H3 10	IT, Latium, Omaro Alto, Montenero Sabino
COI16S 8	COI 13	16S 9	ITS2H3 8	COI 13	16S 9	ITS2 6	H3 9	CS 9	COI 13	16S 9	ITS2 6	H3 9	IT, Latium, Omaro Alto, Montenero Sabino
COI16S 9	COI 10	16S 8	ITS2H3 9	COI 10	16S 8	ITS2 4	H3 9	CS 10	COI 10	16S 8	ITS2 4	H3 9	IT, Latium, Omaro Alto, Montenero Sabino
COI16S 10	COI 19	16S 8											IT, Latium, Omaro Alto, Montenero Sabino
COI16S 11	COI 31	16S 20	ITS2H3 10	COI 31	16S 20	ITS2 11	H3 9	CS 11	COI 31	16S 20	ITS2 11	H3 9	IT, Abruzzi, Carsoli
COI16S 12	COI 32	16S 21											IT, Abruzzi, Carsoli
COI16S 13	COI 8	16S 22											IT, Abruzzi, Carsoli
COI16S 14	COI 8	16S 19	ITS2H3 11	COI 8	16S 19	ITS2 5	H3 9	CS 12	COI 8	16S 19	ITS2 5	H3 9	IT, Abruzzi, Carsoli
COI16S 15	COI 25	16S 14						CS 13	COI 25	16S 14	ITS2 11	H3 9	IT, Latium, Lago del Turano (Castel di Tora, Rieti) [Turz]
COI16S 16	COI 24	16S 13						CS 14	COI 24	16S 13	ITS2 5	H3 9	IT, Latium, Lago del Turano (Castel di Tora, Rieti)
COI16S 17	COI 26	16S 15						CS 15	COI 26	16S 15	ITS2 5	H3 1	IT, Latium, Lago del Turano (Castel di Tora, Rieti)
COI16S 18	COI 20	16S 8						CS 16	COI 20	16S 8	ITS2 5	H3 9	IT, Latium, Lago del Turano (Castel di Tora, Rieti)
COI16S 19	COI 21	16S 10						CS 17	COI 21	16S 10	ITS2 5	H3 1	IT, Latium, Poggio San Lorenzo [Lor]
								CS 18	COI 19	16S 8	ITS2 9	H3 6	IT, Latium, Poggio San Lorenzo
								CS 19	COI 21	16S 10	ITS2 9	H3 6	IT, Latium, Poggio San Lorenzo
			ITS2H3 12	COI 19	16S 8	ITS2 9	H3 6	CS 20	COI 21	16S 10	ITS2 9	H3 11	IT, Latium, Poggio San Lorenzo
			ITS2H3 13	COI 21	16S 10	ITS2 9	H3 11	CS 21	COI 21	16S 10	ITS2 9	H3 11	IT, Latium, Poggio San Lorenzo
			ITS2H3 14	COI 21	16S 10	ITS2 3	H3 1	CS 22	COI 14	16S 8	ITS2 3	H3 1	IT, Latium, Poggio San Lorenzo
COI16S 20	COI 14	16S 8	ITS2H3 15	COI 14	16S 8	ITS2 7	H3 2	CS 23	COI 15	16S 10	ITS2 7	H3 2	IT, Latium, Omaro Alto, Torricella in Sabina [Alt]
COI16S 21	COI 15	16S 10	ITS2H3 16	COI 15	16S 10	ITS2 3	H3 9	CS 24	COI 16	16S 10	ITS2 3	H3 9	IT, Latium, Omaro Alto, Torricella in Sabina
COI16S 22	COI 16	16S 10	ITS2H3 17	COI 16	16S 10	ITS2 7	H3 11	CS 25	COI 16	16S 10	ITS2 7	H3 11	IT, Latium, Omaro Alto, Torricella in Sabina
			ITS2H3 18	COI 16	16S 10	ITS2 8	H3 9	CS 26	COI 16	16S 10	ITS2 8	H3 9	IT, Latium, Omaro Alto, Torricella in Sabina
			ITS2H3 19	COI 18	16S 11	ITS2 5	H3 12	CS 27	COI 18	16S 11	ITS2 5	H3 12	IT, Latium, Omaro Alto, Torricella in Sabina
COI16S 23	COI 18	16S 11						CS 28	COI 30	16S 19	ITS2 11	H3 9	IT, Latium, Valle del Turano (Turania, Rieti) [Tur1]
COI16S 24	COI 17	16S 10						CS 29	COI 27	16S 16	ITS2 11	H3 9	IT, Latium, Valle del Turano (Turania, Rieti)
COI16S 25	COI 30	16S 19						CS 30	COI 27	16S 16	ITS2 12	H3 10	IT, Latium, Valle del Turano (Turania, Rieti)
COI16S 26	COI 27	16S 16	ITS2H3 20	COI 27	16S 16	ITS2 12	H3 10	CS 31	COI 28	16S 17	ITS2 2	H3 1	IT, Latium, Valle del Turano (Turania, Rieti)
			ITS2H3 21	COI 28	16S 17	ITS2 2	H3 1	CS 30	COI 28	16S 17	ITS2 2	H3 1	IT, Latium, Valle del Turano (Turania, Rieti)
COI16S 27	COI 28	16S 17	ITS2H3 22	COI 28	16S 17	ITS2 11	H3 1	CS 31	COI 22	16S 12	ITS2 11	H3 1	IT, Latium, Valle del Turano (Turania, Rieti)

Concatenated sequence	COI haplotype	16S rDNA haplotype	Concatenated sequence	ITS2 common sequence	H3 common sequence	Concatenated sequence	COI haplotype	16S rDNA haplotype	ITS2 common sequence	H3 common sequence	Locality / population
COI16S 28	COI 29	16S 18	CS 32			CS 32	COI 29	16S 18	ITS2 11	H3 1	IT, Latium, Valle del Turano (Turania, Rieti)
			CS 33			CS 33	COI 24	16S 13	ITS2 2	H3 1	IT, Latium, Lago del Turano (Castel di Tor, Rieti) [Tur2]
COI16S 29	COI 22	16S 12	CS 34	ITS2 10	H3 13	CS 34	COI 22	16S 12	ITS2 10	H3 13	IT, Latium, Lago del Turano (Castel di Tor, Rieti)
COI16S 30	COI 23	16S 12									IT, Latium, Lago del Turano (Castel di Tor, Rieti)
COI16S 31	COI 8	16S 6									IT, Vallonia, Monti Reatini [Val]
COI16S 32	COI 7	16S 6									IT, Vallonia, Monti Reatini
COI16S 33	COI 4	16S 4		ITS2H3 24			COI 4	16S 4	ITS2 2	H3 2	IT, Umbria, Monte Fionchi (680 m) [Fio2]
COI16S 34	COI 5	16S 5		ITS2H3 25	H3 2	CS 35	COI 6	16S 2	ITS2 2	H3 2	IT, Umbria, Monte Fionchi (680 m)
COI16S 35	COI 6	16S 2		ITS2H3 26	H3 4	CS 36	COI 5	16S 5	ITS2 3	H3 4	IT, Umbria, Monte Fionchi (680 m)
COI16S 36	COI 3	16S 3		ITS2H3 27	H3 5	CS 37	COI 6	16S 2	ITS2 2	H3 2	IT, Umbria, Monte Fionchi (680 m)
COI16S 37	COI 2	16S 1				CS 38	COI 3	16S 3	ITS2 2	H3 2	IT, Umbria, Monte Fionchi (680 m)
COI16S 38	COI 1	16S 1				CS 39	COI 2	16S 1	ITS2 1	H3 2	IT, Umbria, Monte Fionchi (summit [Fio1])
						CS 40					IT, Umbria, Monte Fionchi (summit)
<i>Monacha cantiana</i> CAN-1											
CAN-1	MG208916	MG208987	CAN-1	MHI137974	MG209046	CS 41	MG208916	MG208987	MHI137974	MG209046	IT, Latium, Valle dell'Aniene, Rome
	MG208915	MG208985		MHI137973	MG209045	CS 42	MG208915	MG208985	MHI137973	MG209045	IT, Latium, Valle dell'Aniene, Rome
	MG208917	MG208989		MHI137975	MG209047	CS 43	MG208917	MG208989	MHI137975	MG209047	IT, Latium, Valle dell'Aniene, Rome
	MG208905	MG208977				CS 44	MG208905	MG208977	MHI137972	MG209039	IT, Latium, Gole del Velino
	MG208906	MG208979									IT, Latium, Gole del Velino
	MG208910	MG208978									IT, Latium, Gole del Velino
	MG208921	MG208990				CS 45	MG208921	MG208990	MHI137976	MG209043	IT, Latium, Valle del Tronto
	MG208923	MG208994		MHI137978	MG209048	CS 46	MG208923	MG208994	MHI137978	MG209048	IT, Latium, Valle del Tronto
	MG208884	MG208966				CS 47	MG208884	MG208966	MHI137963	MG209031	UK, Barrow near Barnsley
	MG208899	MG208976		MHI137971	MG209038	CS 48	MG208899	MG208976	MHI137971	MG209038	UK, Rotherham
	MG208893	MG208960									UK, Rotherham
	MG208898	MG208975		MHI137969	MG209037	CS 49	MG208898	MG208975	MHI137969	MG209037	UK, Sheffield
	MG208904	MG208971									UK, Sheffield
	MG208891	MG208972									UK, Cambridge
<i>Monacha cantiana</i> CAN-2											
CAN-2	MG208925	MG208996	CAN-2	MK067000	MG209050						IT, Venetum, Sorga
	MG208926	MG209001									IT, Venetum, Sorga
	MG208928	MG208998									IT, Venetum, Sorga
	MG208932	MG209003		MHI137981	MG209052	CS 50	MG208932	MG209003	MHI137981	MG209052	IT, Lombardy, Rezzato
<i>Monacha cantiana</i> s. l. CAN-3 (<i>Monacha</i> sp.)											
CAN-3	MG208936	MG209009	CAN-3	MHI137983	MG209055	CS 51	MG208936	MG209009	MHI137983	MG209055	AU, Breitenlee
	MG208938	MG209008									AU, Breitenlee
	MG208933	MG209007		MHI137982	MG209054	CS 52	MG208933	MG209007	MHI137982	MG209054	IT, Emilia Romagna, Fiume Setta
	MG208934	MG209005									IT, Emilia Romagna, Fiume Setta
	MG208935	MG209006									IT, Emilia Romagna, Fiume Setta

Concatenated sequence	COI haplotype	16S rDNA haplotype	Concatenated sequence	ITS2 common sequence	H3 common sequence	Concatenated sequence	COI haplotype	16S rDNA haplotype	ITS2 common sequence	H3 common sequence	Locality / population
<i>Monacha cantiana</i> s. l. CAN-4 (<i>Monacha cemenelca</i>)											
CAN-4	MG208939	MG209011	CAN-4	MH137984	MG209058	CS 53	MG208939	MG209011	MH137984	MG209058	FR, Alpes-Maritimes, Sainte Thecle
	MG208940	MG209012									FR, Alpes-Maritimes, Sainte Thecle
	MG208941	MG209013									FR, Alpes-Maritimes, Sainte Thecle
<i>Monacha cantiana</i> s. l. CAN-5 (<i>Monacha</i> sp.)											
CAN-5	MK066929	MK066947	CAN-5								IT, Tuscany, Foce di Pianza
	MK066933	MK066951									IT, Tuscany, Foce di Pianza
				CS 54	MK066966		MK066931	MK066949	MK066982	MK066967	IT, Tuscany, Foce di Pianza
				CS 55	MK066983		MK066930	MK066948	MK066981	MK066966	IT, Tuscany, Foce di Pianza
				CS 56	MK066968		MK066932	MK066950	MK066983	MK066968	IT, Tuscany, Foce di Pianza
				CS 57	MK066987		MK066935	MK066954	MK066987	MK066974	IT, Tuscany, Campo Cecina
				CS 58	MK066989		MK066937	MK066956	MK066989	MK066974	IT, Tuscany, Campo Cecina
				CS 59	MK066985		MK066934	MK066952	MK066985	MK066970	IT, Tuscany, Campo Cecina
				CS 60	MK066988		MK066936	MK066955	MK066988	MK066973	IT, Tuscany, Campo Cecina
				CS 61	MK066976		MK066938	MK066957	MK066991	MK066976	IT, Piastra
											IT, Piastra
											IT, Piastra
<i>Monacha cantiana</i> s. l. CAN-6 (<i>Monacha</i> sp.)											
CAN-6	MK066942	MK066960	CAN-6								IT, Tuscany, Campagrina
	MK066943	MK066961									IT, Tuscany, Campagrina
	MK066944	MK066962				CS 62	MK066944	MK066962	MK066997	MK066978	IT, Tuscany, Campagrina
	MK066945	MK066963				CS 63	MK066946	MK066964	MK066999	MK066980	IT, Tuscany, Campagrina
<i>Monacha parmeciana</i> PAR											
PAR	MG208946	MG209019	PAR								IT, Basilicata, Moliterno to Fontana d'Eboli
	MG208947	MG209016									IT, Basilicata, Moliterno to Fontana d'Eboli
				CS 64	MG209061		MG208944	MG209017	MK067005	MG209061	IT, Basilicata, Moliterno to Fontana d'Eboli
				CS 65	MG209067		MG208949	MG209020	MH137987	MG209067	IT, Basilicata, Moliterno to Fontana d'Eboli
											IT, Tuscany, Nievole
											IT, Tuscany, Nievole & Arezzo
											IT, Tuscany, Arezzo
											IT, Tuscany, Arezzo
											IT, Tuscany, Arezzo
											IT, Tuscany, Arezzo & La Casella
<i>Monacha cartisiana</i> CAR											
CAR	MH203998	MH204081	CAR	MH137993	MG209072	CS 68	KM247376	KM247391	MH137993	MG209072	DE, Lower Saxony, Hannover, Schinde
											HU, Kis-Balaton

0.1 mm using ADOBE PHOTOSHOP 7.0.1 on digital images of apertural and umbilical standard views taken with a Canon EF 100 mm 1:2.8 L IS USM macro lens mounted on a Canon F6 camera: **AH** aperture height, **AW** aperture width, **LWfW** last whorl final width, **LWmW** last whorl medial width, **LWah** height of adapical sector of last whorl, **LWmH** height of medial sector of last whorl, **PWH** penultimate whorl height, **PWfW** penultimate whorl final width, **PWmW** penultimate whorl medial width, **SD** shell diameter, **SH** shell height, and **UD** umbilicus diameter (Pieńkowska et al. 2018a: fig. 1).

One hundred and thirty-five specimens of *M. pantanellii*, *M. cantiana* s. l. (with its six molecular lineages), *M. parumcincta* and *M. cartusiana* were analysed to examine anatomical variability between species; the 50 specimens of ten populations of *M. pantanellii* were also considered to investigate genital variability between populations of this species (see Table 1 and Pieńkowska et al. 2018a, 2019b). Snail bodies were dissected under the light microscope (Wild M5A or Zeiss SteREO Lumar V12). Anatomical details were drawn using a Wild camera lucida. Acronyms: **BC** bursa copulatrix, **BW** body wall, **DBC** duct of bursa copulatrix, **DG** digitiform glands (also known as mucous glands), **E** epiphallus (from base of flagellum to beginning of penial sheath), **F** flagellum, **FO** free oviduct, **GA** genital atrium, **GAR** genital atrium retractor, **OSD** ovispermiduct, **P** penis, **PP** penial papilla (also known as glans), **V** vagina, **VA** vaginal appendix (also known as appendicula), **VAS** vaginal appendix basal sac, **VS** vaginal sac (only present in *M. cartusiana*; see Pieńkowska et al. 2015: figs 11, 12), **VD** vas deferens. Seven anatomical variables (DBC, E, F, P, V, VS, VA) were measured under a light microscope (0.01 mm) using callipers (see: Pieńkowska et al. 2018a: fig. 2).

Detailed methods of multivariate ordination by Principal Component Analysis (PCA) and Redundancy Analysis (RDA), performed on the original shell and genitalia matrices as well as on the shape-related Z-matrices, are described in a previous paper (Pieńkowska et al. 2018a).

Differences between species for each shell and genital character were assessed through box-plots and descriptive statistics. Overall significance of differences was obtained using the Kruskal-Wallis test; when the test proved significant, multiple comparisons between pairs of species were performed using Dunn's test. In order to control the false discovery rate (FDR), the Benjamini-Hochberg correction was used to adjust P-values for multiple comparisons. The `dunn.test` function with the `alt = TRUE` option and $\alpha = 0.01$ in the `dunn.test` R package were used for analysis (Dinno 2017).

Results

Molecular study

DNA sequencing resulted in 53 and 57 sequences of mitochondrial COI and 16S rDNA as well as 43 and 57 sequences of nuclear ITS2 and H3 gene fragments, respectively. They were all deposited in GenBank as MT380011–MT380063 (COI), MT376031–

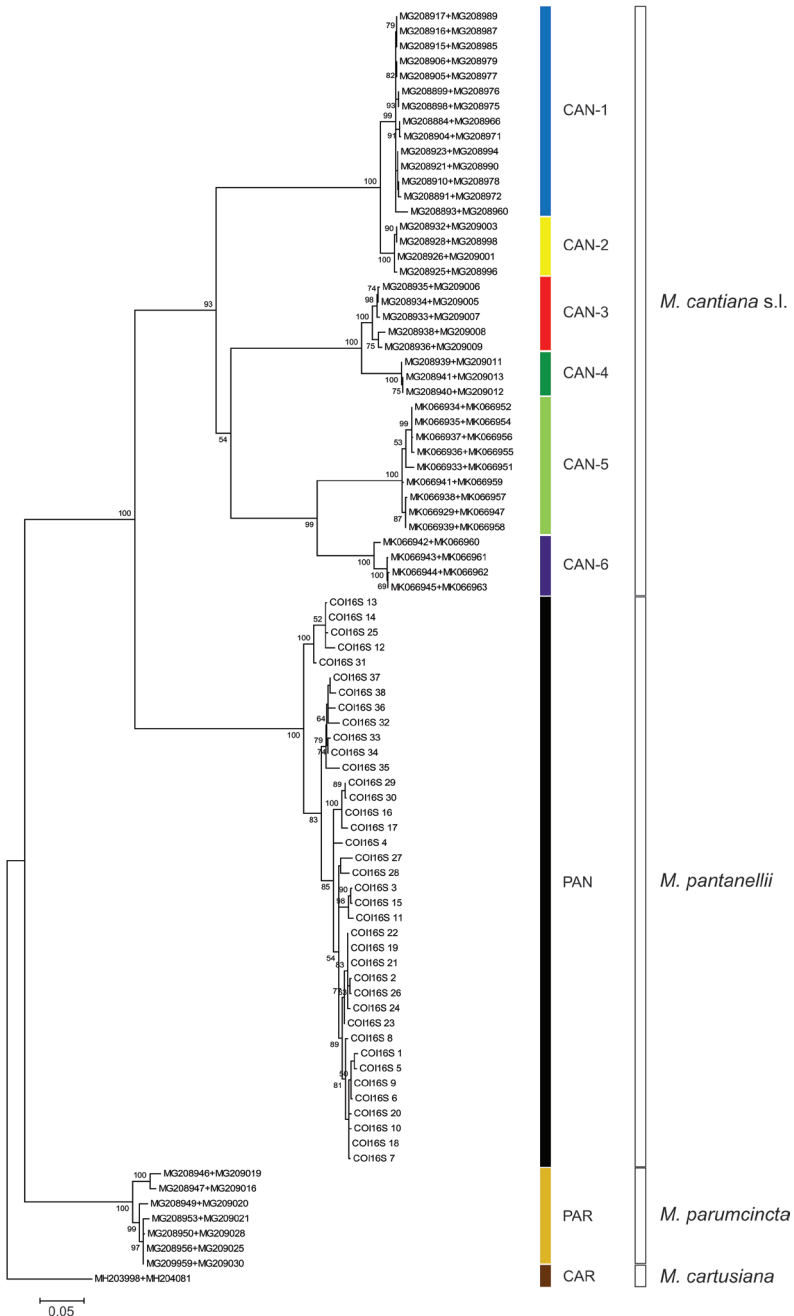


Figure 2. Maximum Likelihood (ML) tree of concatenated COI and 16S rDNA haplotypes of *Monacha pantanellii* (see Table 4). New COI and 16S rDNA sequences of *M. pantanellii* (Table 1) were compared with COI and 16S rDNA sequences of *M. cantiana* s. l. and *M. parumcincta* obtained from GenBank (Tables 2, 4). Numbers next to branches indicate bootstrap support above 50% calculated on 1000 replicates (Felsenstein 1985). The tree was rooted with *M. cartusiana* concatenated sequences obtained from GenBank (Table 2).

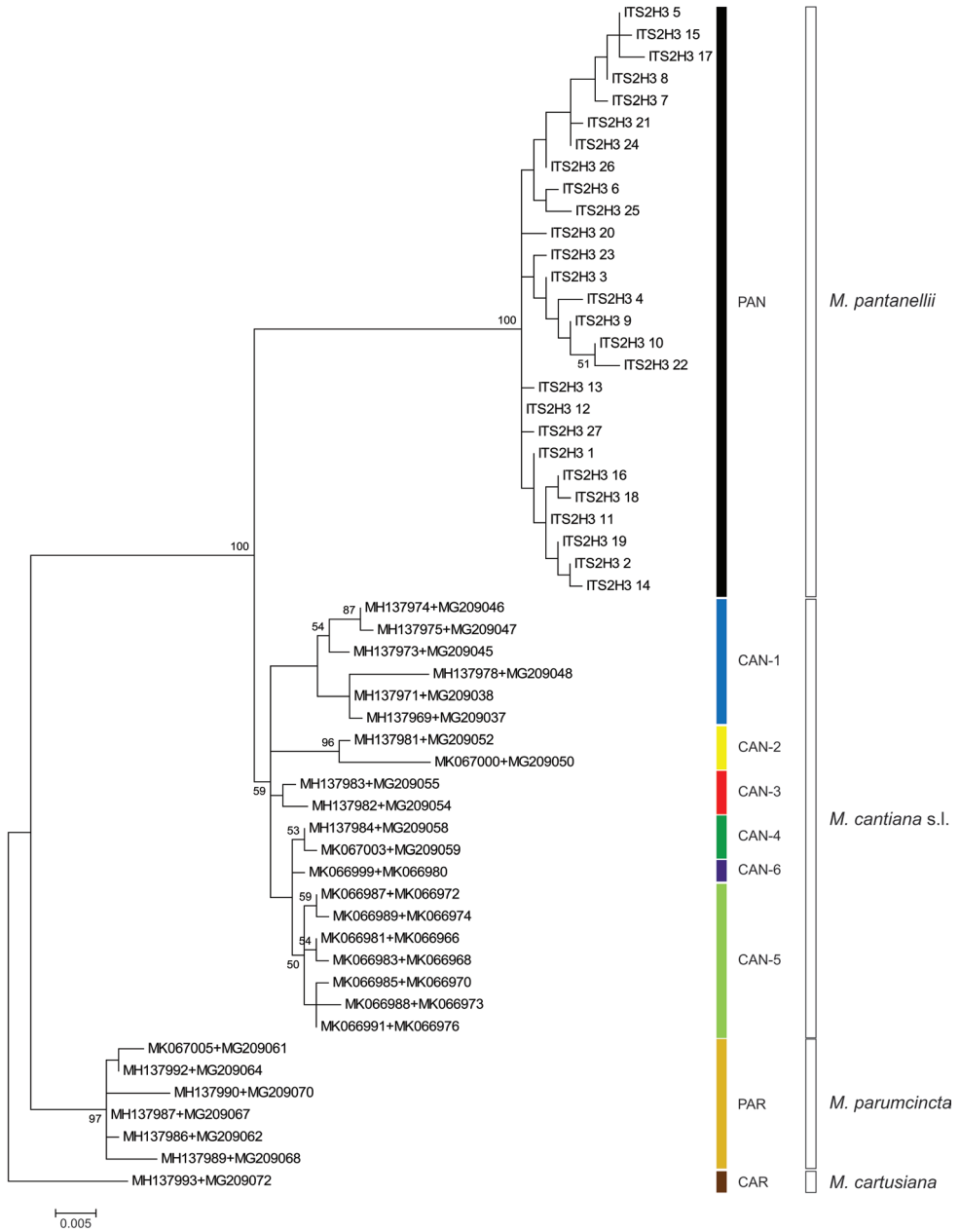


Figure 3. Maximum Likelihood (ML) tree of concatenated ITS2 and H3 common sequences of *Monacha pantanellii* (see Table 4). New ITS2 and H3 sequences of *M. pantanellii* (Table 1) were compared with ITS2 and H3 sequences of *M. cantiana* s. l. and *M. parumcincta* obtained from GenBank (Tables 2, 4). Numbers next to branches indicate bootstrap support above 50% calculated on 1000 replicates (Felsenstein 1985). The tree was rooted with *M. cartusiana* concatenated sequences obtained from GenBank (Table 2).

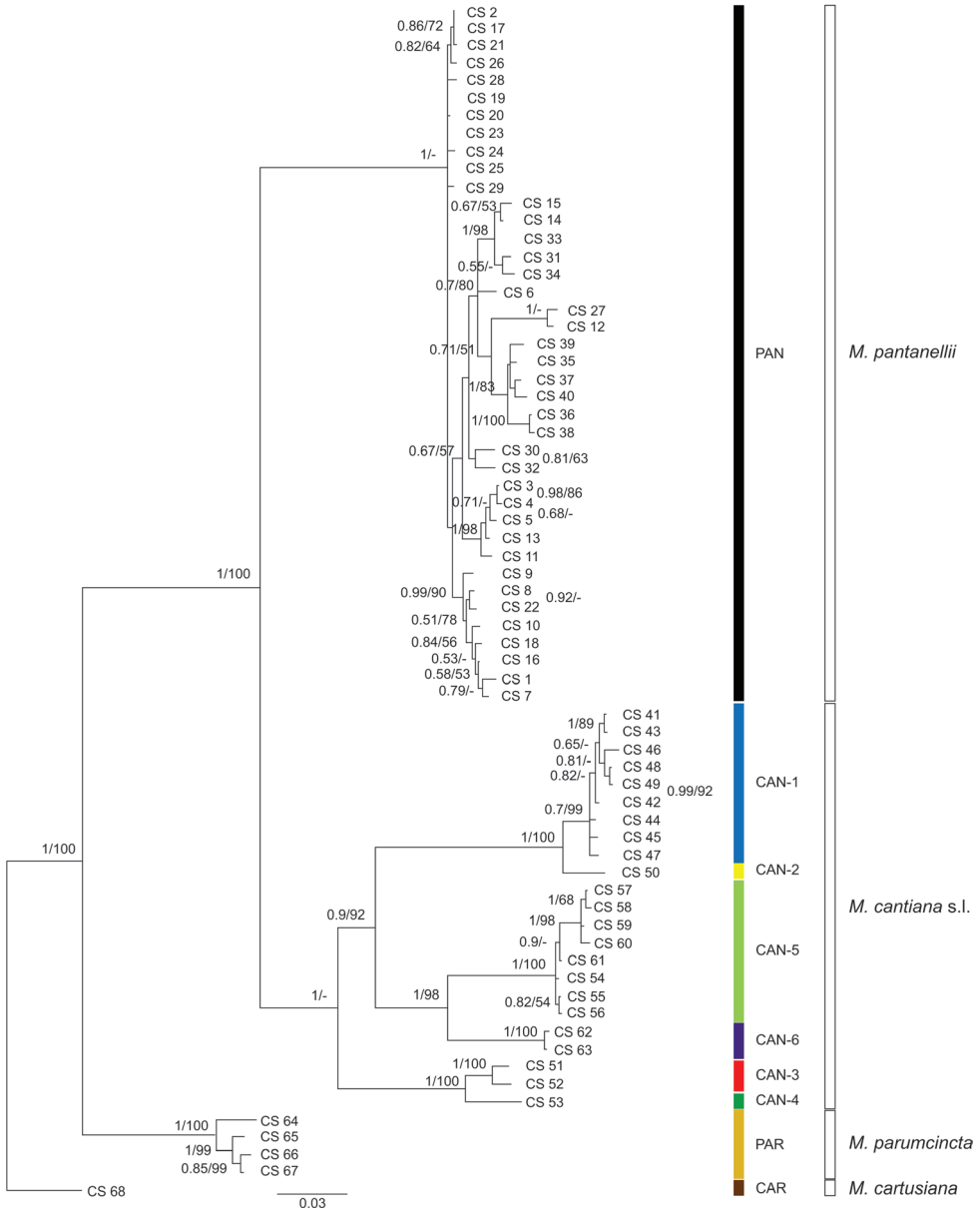


Figure 4. Bayesian 50% majority-rule consensus tree of the concatenated data set of COI and 16S rDNA haplotypes, and ITS2 and H3 common sequences (see Table 4). Sequences of *M. pantanellii* were compared with appropriate sequences of *M. cantiana* s. l. and *M. parumcincta* obtained from GenBank (Tables 2, 4). Posterior probabilities (left) and bootstrap support above 50% from ML analysis (right) are indicated next to the branches. Bootstrap analysis was run with 1000 replicates (Felsenstein 1985). The tree was rooted with *M. cartusiana* concatenated sequences obtained from GenBank (Table 2).

MT376087 (16S rDNA), MT376088–MT376130 (ITS2) and MT385776–MT385832 (H3) (Table 1). Thirty-six COI (COI 1–COI 36) and 25 16S rDNA (16S 1–16S 25) haplotypes, as well as 15 ITS2 (ITS2 1–ITS2 15) and 15 H3 (H3 1–H3 15) common sequences were recognised among them (Table 1). They were used for phylogenetic analysis with appropriate sequences representing *M. parumcincta* (PAR) and *M. cartusiana* (CAR), as well as six molecular lineages of *M. cantiana* s. l. (CAN-1–CAN-6) obtained from GenBank (Table 2). ML trees for concatenated sequences of mitochondrial COI and 16S rDNA (Fig. 2, Table 4) and of nuclear ITS2 and H3 (Fig. 3, Table 4) gene fragments, as well as the Bayesian Inference (BI) phylogenetic tree of concatenated sequences of COI+16S rDNA+ITS2+H3 gene fragments (Fig. 4, Table 4) clustered the concatenated sequences in one clade (PAN) separated from all other clades hitherto recognised for *M. cantiana* s. l. (CAN-1, CAN-2, CAN-3, CAN-4, CAN-5, CAN-6), *M. parumcincta* (PAR) and *M. cartusiana* (CAR) populations (Pieńkowska et al. 2018a, 2018b, 2019b).

K2P genetic distances between COI haplotypes are summarised in Table 5. Differences in COI haplotypes of *M. pantanellii* are rather small (up to 4.5%). Three varied somewhat more (COI 8 from populations from Vallonina [Val] and Carsoli [Car], COI 30 from Valle del Turano [Tur1] and COI 32 from Carsoli [Car]), bringing the mean for all populations to 0.2–6.7%. It was not possible to differentiate one population from the others. It is noteworthy that haplotypes of *M. pantanellii* are very different (15.5–22.0%) from the others representing *M. cantiana* s. l. (i.e., *M. cantiana* CAN-1–CAN-3, *M. ceme-nelea* (Risso, 1826) CAN-4, and *M. sp.* CAN-5–CAN-6) as well as from *M. parumcincta* (18.1–21.4%) and *M. cartusiana* (16.6–18.3%) (Pieńkowska et al. 2018a, 2019b).

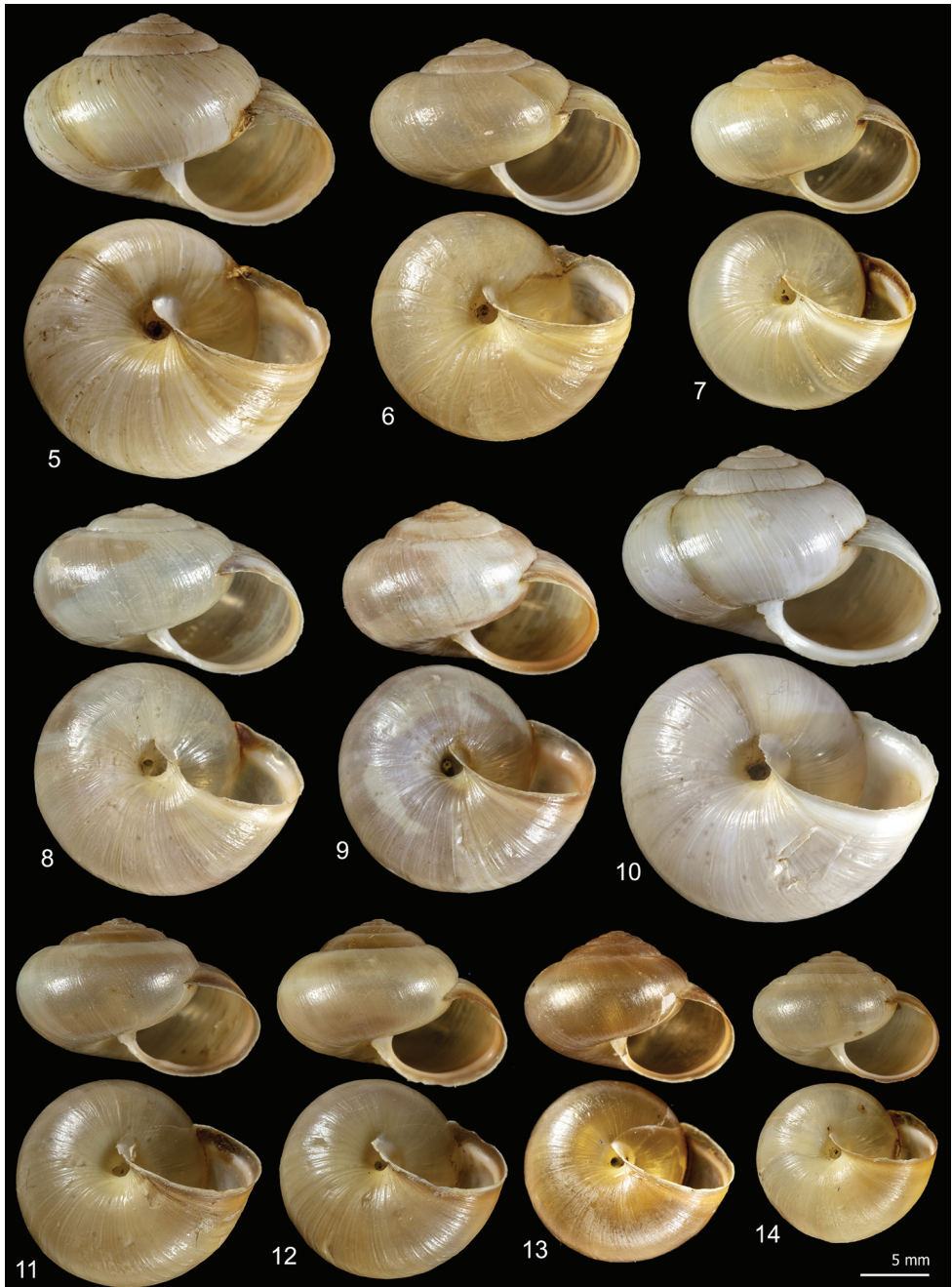
Table 5. Ranges of K2P genetic distances between analysed COI sequences.

Comparison	COI (%)
Within <i>M. pantanellii</i> PAN	0.2–6.7
Between <i>M. pantanellii</i> PAN and <i>M. cantiana</i> CAN-1	17.2–21.2
Between <i>M. pantanellii</i> PAN and <i>M. cantiana</i> CAN-2	19.1–22.0
Between <i>M. pantanellii</i> PAN and <i>M. cantiana</i> s. l. CAN-3 (<i>M. sp.</i>)	16.8–18.9
Between <i>M. pantanellii</i> PAN and <i>M. cantiana</i> s. l. CAN-4 (<i>M. ceme-nelea</i>)	15.5–17.4
Between <i>M. pantanellii</i> PAN and <i>M. cantiana</i> s. l. CAN-5 (<i>M. sp.</i>)	17.1–19.9
Between <i>M. pantanellii</i> PAN and <i>M. cantiana</i> s. l. CAN-6 (<i>M. sp.</i>)	15.5–18.6
Between <i>M. pantanellii</i> PAN and <i>M. parumcincta</i> PAR	18.1–21.4
Between <i>M. pantanellii</i> PAN and <i>M. cartusiana</i> CAR	16.6–18.3

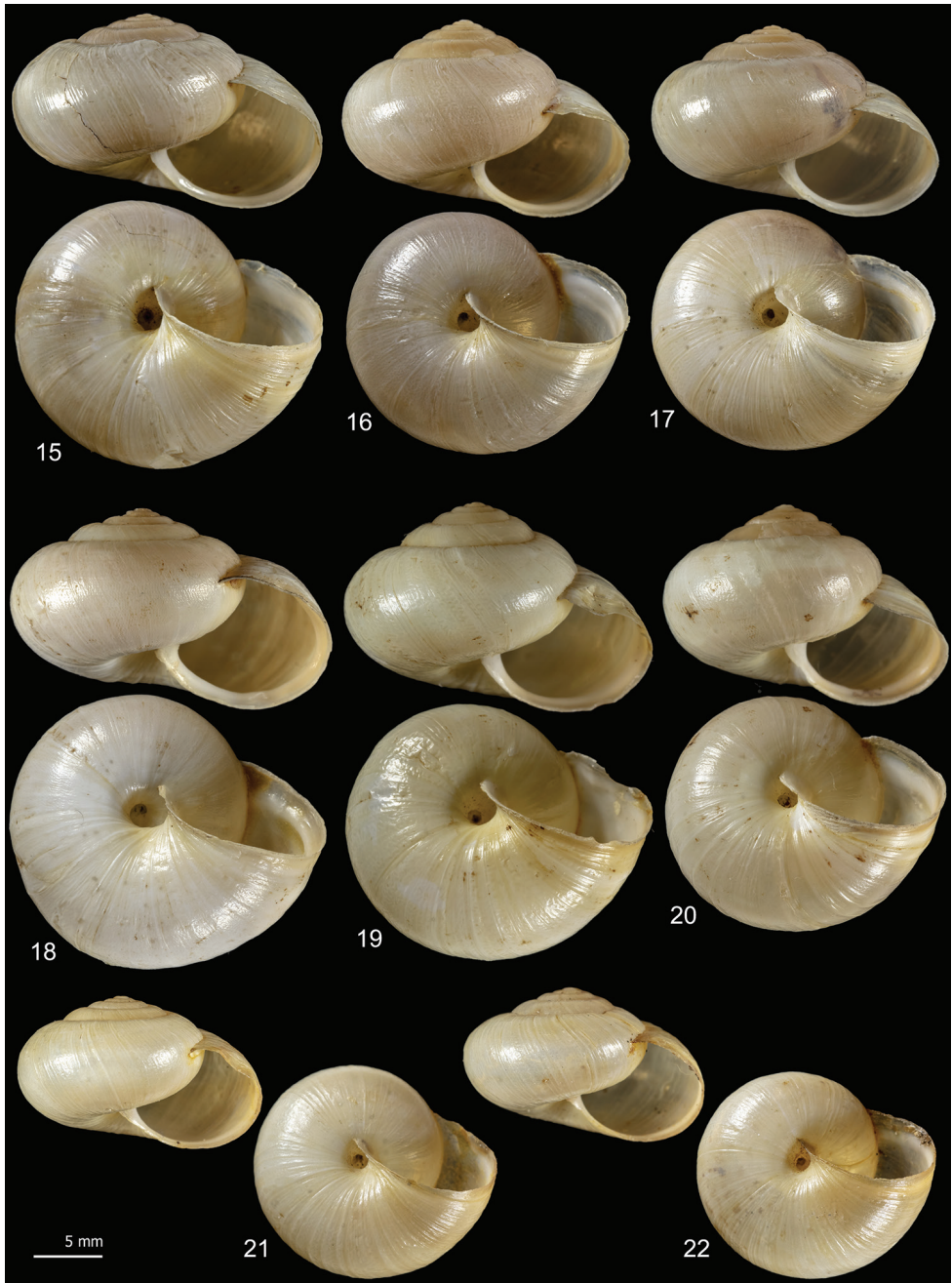
Morphological study: shell

Monacha pantanellii has a globose to sub-globose shell, variable in size, colour, and presence of paler subsutural and peripheral bands, with roundish to oval slightly descending aperture, a brownish peristome and a very small to small umbilicus (Figs 5–31).

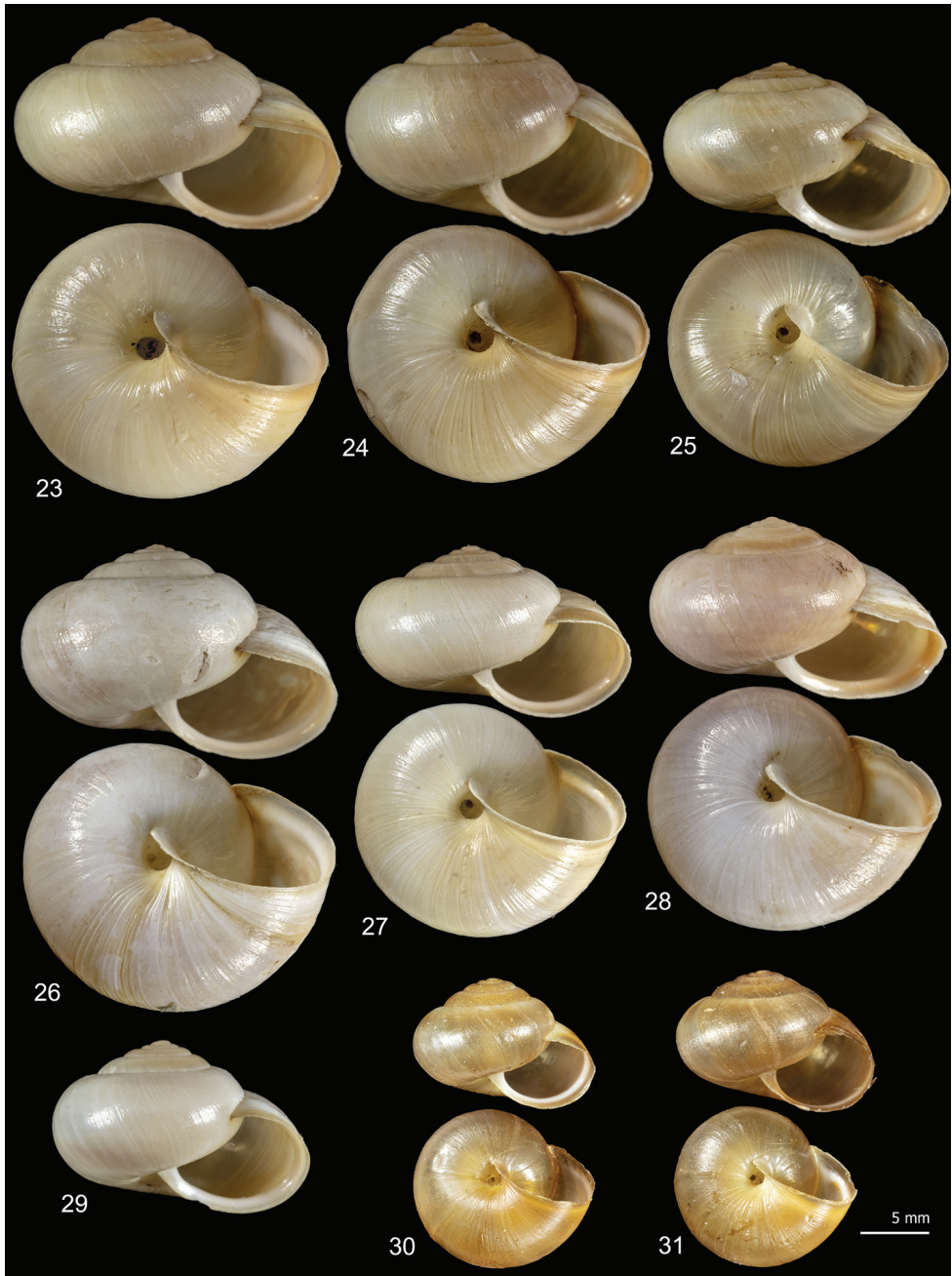
RDA with species or molecular lineage constraint on the shape and size matrix (Fig. 32) showed that RDA 1 (33%, $P < 0.001$) separated all the species or molecular lineages from PAR. The preliminary classic PCA revealed size as the first major source of morphological variation, since PC1 (70%) was a positive combination of all variables. On



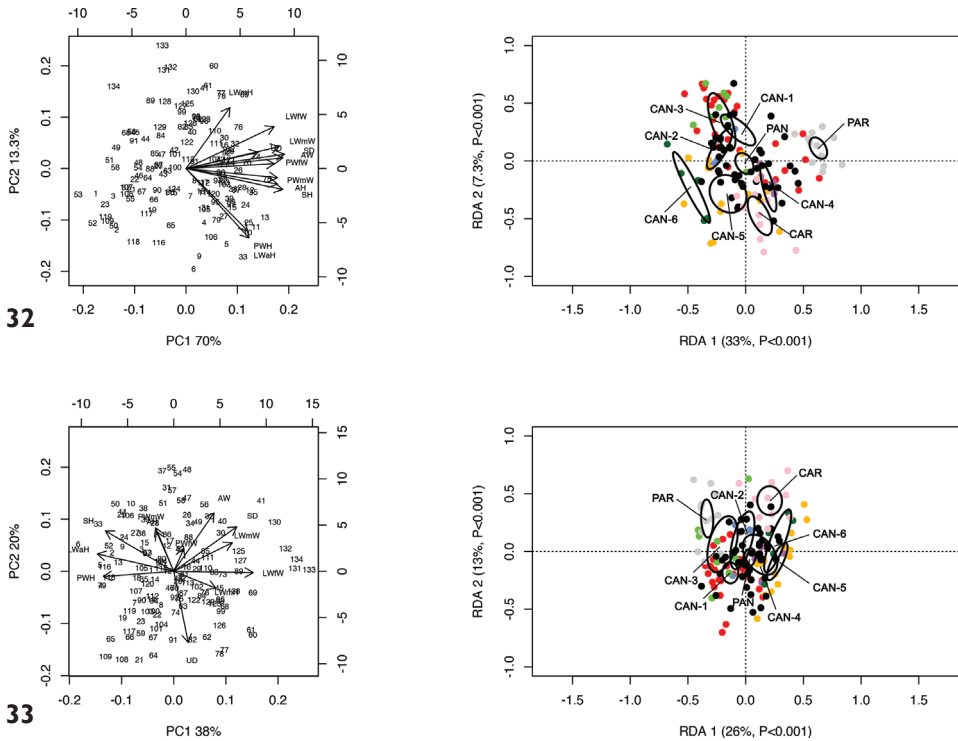
Figures 5–14. Shell variability in *Monacha pantanellii* from Monte Fionchi, summit [Fio1] (FGC 8140) (**5, 6**), Monte Fionchi, Torrecola [Fio2] (FGC 38944) (**7**), road to Montenero Sabino [Sab] (FGC 41552) (**8–10**) and Turania [Tur1] (FGC 42971) (**11–14**).



Figures 15–22. Shell variability in *Monacha pantanellii* from Lago del Turano [Tur2] (FGC 41654) (**15–17**), Via Salaria, Ornaro Alto [Alt] (FGC 41553) (**18–20**) and Vallonina [Val] (FGC 25345) (**21, 22**).



Figures 23–31. Shell variability in *Monacha pantanellii* from Via Salaria, Poggio San Lorenzo [Lor] (FGC 41551) (**23–25**), Valle dell’Aniene, Roccagiovine [Ani] (FGC 42974) (**26–29**) and Carsoli [Car] (FGC 41651(**30, 31**)).



Figures 32, 33. Principal component analysis (PCA) and Redundancy analysis (RDA) with species or molecular lineage constraint applied to the original shell matrix (**32**) and shape-related Z-matrix (**33**).

the contrary, RDA 2 (7.3%, $P < 0.001$) slightly separated CAN-1, CAN-2 and CAN-3 from CAN-4, CAN-5, CAN-6 and PAN with PAR in intermediate position. In this regard, PC2 (13%) mostly accounted for contrast between LWmH vs. LWaH and PWH.

RDA on the shape (Z) matrix (Fig. 33) showed a hazier separation of species or molecular lineages, confirming that size is a major source of morphological variation, although both RDA axes proved to be significant. In particular, RDA 1 separated CAR, CAN-5, CAN-6 from PAR, CAN-1 and CAN-3, with the other groups in a more or less intermediate position. Conversely, RDA 2 separated PAR and CAR from all the other species or molecular lineages. Shape-related PCA indicated that SH, LWaH and PWH vs. LWfW were the principal shape determinants on PC1 and PWmW, AH and AD vs. UD on PC2.

Box plots (Fig. 34) proved that the shell characters only have discriminating value in distinguishing *Monacha pantanellii* from other species or molecular lineages in a few cases. In fact, according to Dunn’s test with Benjamini-Hochberg adjustment ($\alpha = 0.01$), no character significantly distinguished PAN from CAN-1, CAN-2 and CAN-4, only one distinguished it from CAN-5 (UD), only two from CAR (LWah, PWH), four from CAN-6 (SD, LWmW, LWfW, UD), six from CAN-3 (SH, AH, SD, AD,

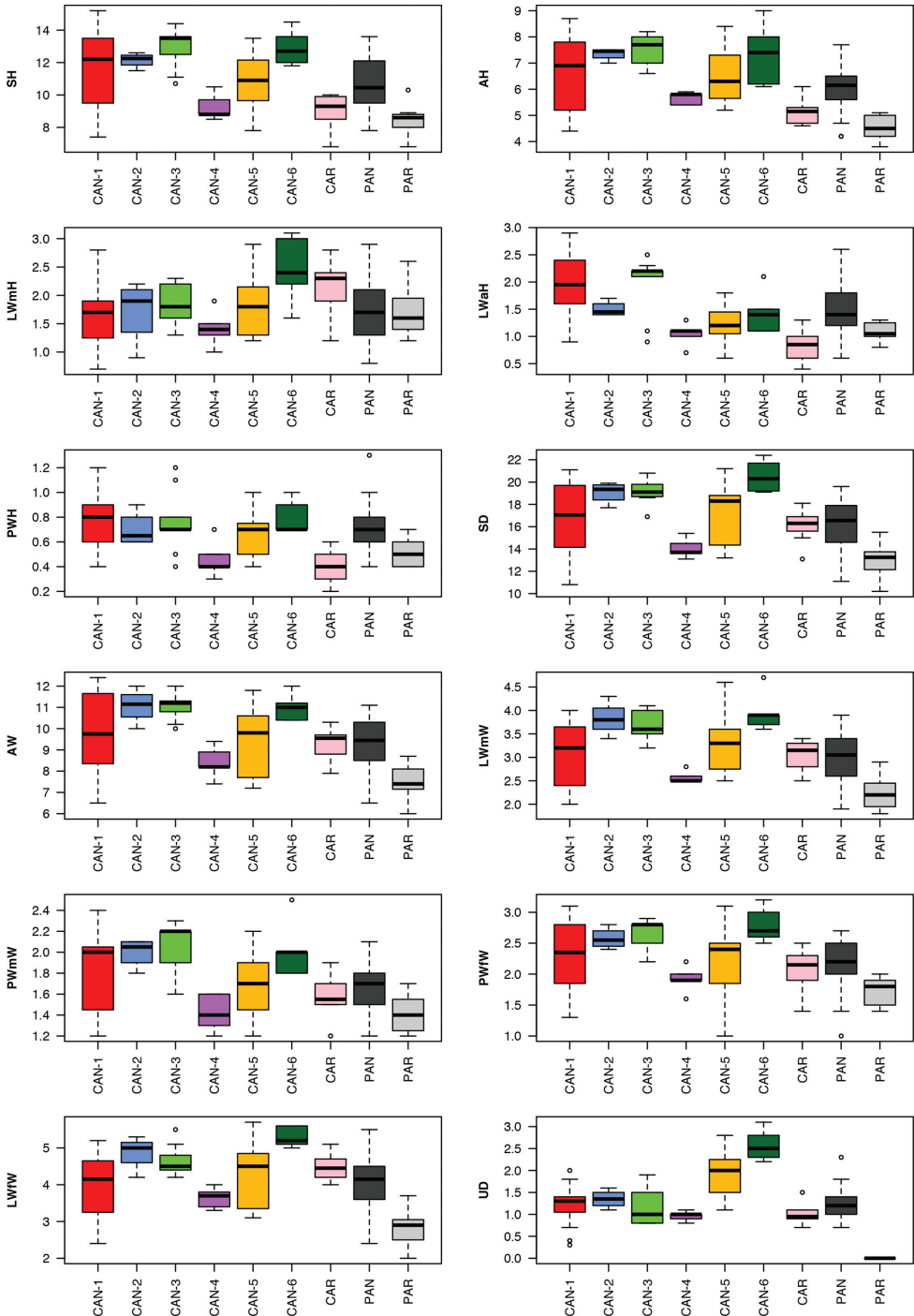


Figure 34. Box plots for shell characters of the nine *Monacha* species or molecular lineages investigated. The lower and upper limits of the rectangular boxes indicate the 25th to 75th percentile range, and the horizontal line within the boxes is the median (50th percentile).

Table 6. Results of Dunn's test with Benjamini-Hochberg correction ($\alpha = 0.01$) for shell and genital characters (in bold $P \leq 0.01$).

Pairs	SH	AH	LWmH	LWaH	PWH	SD	
PAN vs. CAN-1	0.0956	0.1431	0.3784	0.0134	0.1993	0.2703	
PAN vs. CAN-2	0.2257	0.0763	0.9541	0.8128	0.9275	0.0517	
PAN vs. CAN-3	0.0075	0.0039	0.7552	0.1309	0.6223	0.0063	
PAN vs. CAN-4	0.1428	0.4689	0.3232	0.0750	0.0467	0.1496	
PAN vs. CAN-5	0.8439	0.4087	0.8724	0.1396	0.8163	0.3364	
PAN vs. CAN-6	0.0514	0.0895	0.1007	0.8442	0.3559	0.0039	
PAN vs. CAR	0.0468	0.0330	0.1163	0.0009	0.0026	0.7972	
PAN vs. PAR	0.0022	0.0003	0.7724	0.0110	0.0227	0.0044	
Pairs	AW	LWmW	PWmW	PWfW	LWfW	UD	
PAN vs. CAN-1	0.1792	0.5046	0.0468	0.4863	0.8655	0.9405	
PAN vs. CAN-2	0.0488	0.0189	0.0434	0.1789	0.0826	0.5901	
PAN vs. CAN-3	0.0054	0.0046	0.0085	0.0265	0.0711	0.5962	
PAN vs. CAN-4	0.3094	0.1947	0.1515	0.1979	0.3344	0.1765	
PAN vs. CAN-5	0.8931	0.2051	0.7961	0.8167	0.3478	0.0015	
PAN vs. CAN-6	0.0330	0.0043	0.0434	0.0249	0.0030	0.0029	
PAN vs. CAR	1.0000	0.9480	0.4609	0.4984	0.1652	0.1370	
PAN vs. PAR	0.0046	0.0028	0.0365	0.0054	0.0008	0.0000	
Pairs	DBC	V	F	E	P	VA	VS
PAN vs. CAN-1	0.3802	0.0992	0.0000	0.0072	0.0001	0.0000	1.0000
PAN vs. CAN-2	0.0808	0.1870	0.0001	0.0003	0.5535	0.0000	1.0000
PAN vs. CAN-3	0.9561	0.4778	0.0000	0.0057	0.5350	0.0000	1.0000
PAN vs. CAN-4	0.3528	0.9287	0.0708	0.9913	0.0001	0.0013	1.0000
PAN vs. CAN-5	0.0813	0.1862	0.6815	0.0002	0.0006	0.0001	1.0000
PAN vs. CAN-6	0.1163	0.3350	0.7574	0.0328	0.0101	0.0001	1.0000
PAN vs. CAR	0.0009	0.2609	0.0000	0.0122	0.0000	0.6581	0.0000
PAN vs. PAR	0.0430	0.0000	0.0000	0.1266	0.0000	0.5918	1.0000

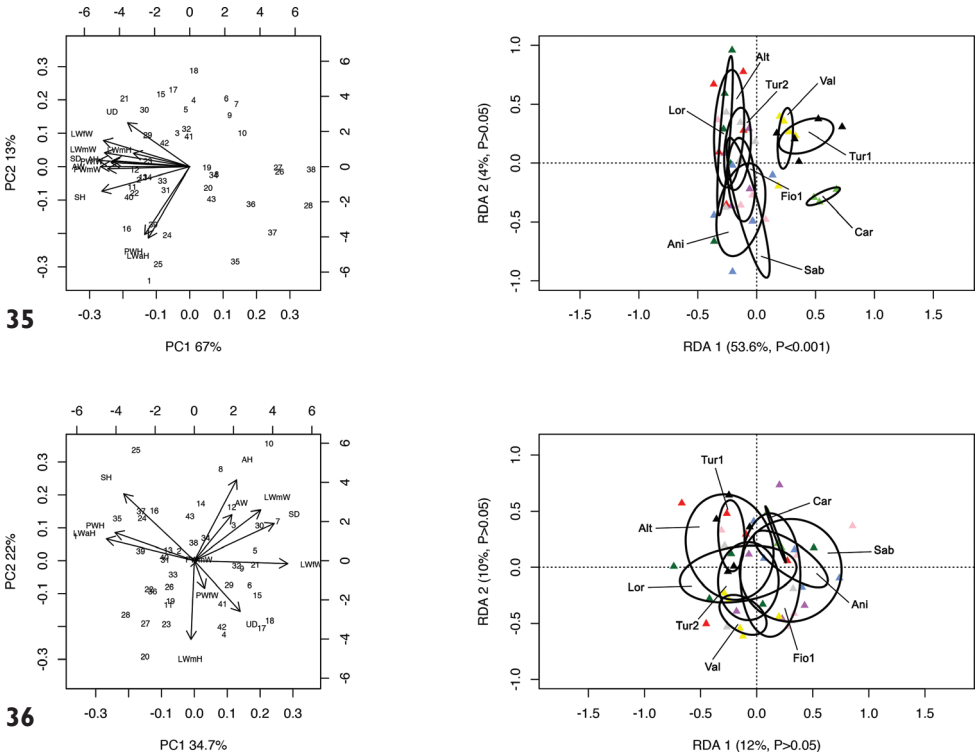
LWmW, PWmW) and eight from PAR (SH, AH, SD, AD, LWmW, PWfW, LWfW, UD) (Table 6).

RDA with population constraint on the shape and size matrix (Fig. 35) showed that RDA 1 (53.6%, $P < 0.001$) separated them into two groups, the first, including populations from Via Salaria, Ornaro Alto [Alt], Valle dell'Aniene, Roccagiovine [Ani], Monte Fionchi, summit [Fio1], Via Salaria, Poggio San Lorenzo [Lor], Montero Sabino [Sab] and Lago del Turano [Tur2] was separate from the second consisting of populations from Carsoli [Car], Turania [Tur1] and Vallonina [Val]. On the contrary, RDA 2 (4.0%, $P > 0.05$) showed no significant separation of populations. The preliminary classic PCA revealed size as the first major source of morphological variation, since PC1 (67.0%) was a negative combination of all variables.

RDA on the shape (Z) matrix (Fig. 36) showed no significant separation between populations, again confirming that size is a major source of morphological variation. Shape-related PCA indicated that LWaH and PWH vs. LWfW were the two principal shape determinants on PC1 and AH vs. LWmH on PC2.

Morphological study: anatomy

Monacha pantanellii has distal genitalia very similar to those of the *Monacha cantiana* group. The most remarkable features are the usually short vaginal appendix with mid or proximal vaginal insertion, the long flagellum and the penial papilla with thick

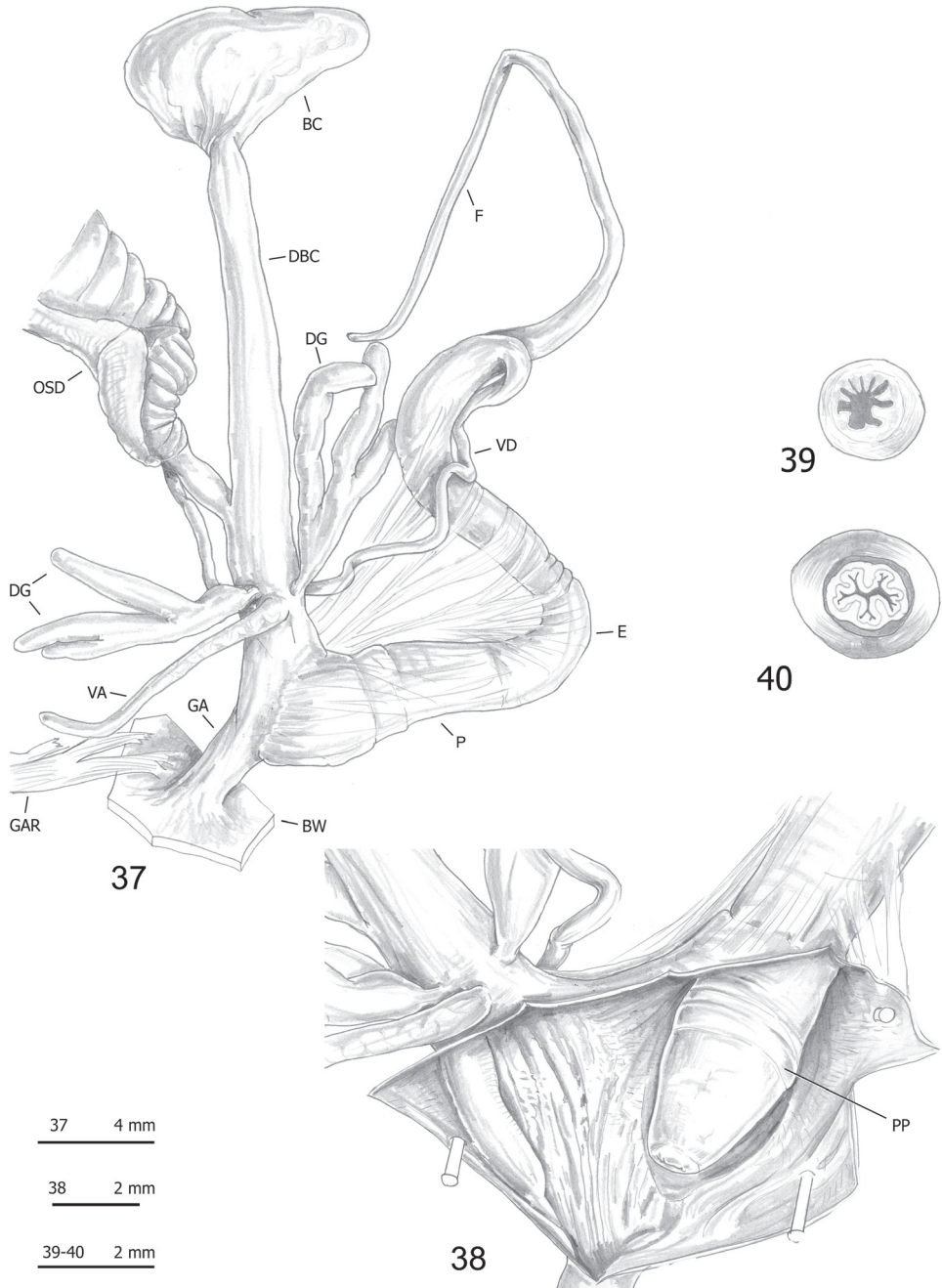


Figures 35, 36. Principal component analysis (PCA) and Redundancy analysis (RDA) with population constraint applied to the original shell matrix (**35**) and shape-related Z-matrix (**36**) of specimens of *Monacha pantanellii*.

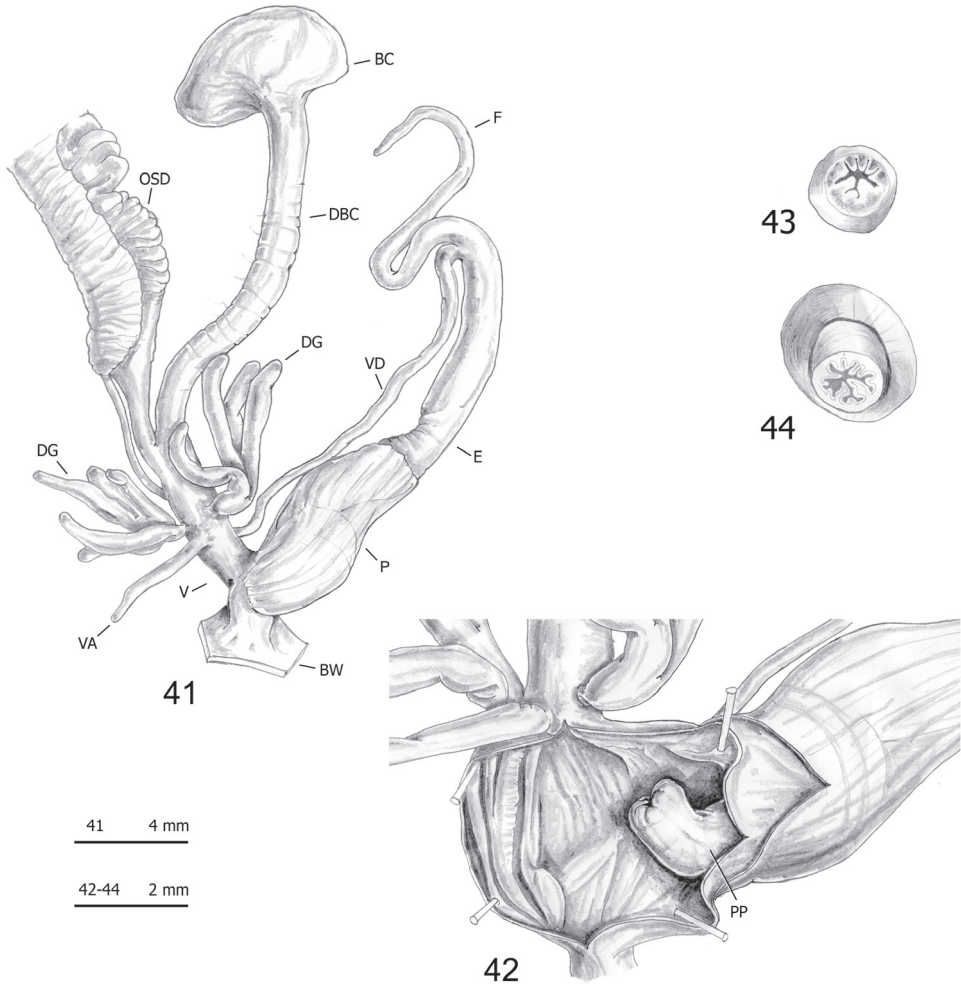
external wall bordering a central duct without strips joining it to the external wall and with a lumen filled by many variably sized pleats (Figs 37–63).

RDA with species or molecular lineage constraint on the shape and size matrix (Fig. 64) showed that RDA 1 (27%, $P < 0.001$) separated *M. cantiana* s. l. (CAN-1, CAN-2, CAN-3, CAN-4, CAN-5 and CAN-6) from PAN, PAR and CAR. The preliminary classic PCA revealed size as the first major source of morphological variation, since PC1 (43%) accounted for VS vs. all the other variables. On the contrary, RDA 2 (22%, $P < 0.001$) separated CAN-5, CAN-6 and PAN from CAR and PAR. The group CAN-1, CAN-2, CAN-3 and CAN-4 was in intermediate position. In that regard, PC2 (20%) accounted for a contrast between E and VA vs. F, P, V and VS.

RDA with species or molecular lineage constraint on the shape (Z) matrix (Fig. 65) showed that RDA 1 (43%, $P < 0.001$) separated PAN from the group CAN-1, CAN-2, CAN-3, CAN-4 and CAN-6, with CAN-5, PAR and CAR in intermediate position, and that RDA 2 (20%, $P < 0.001$) separated CAR from all the others. Shape-related PCA indicated that VA and E vs. V and P were the principal shape determinants on PC1 and VS and V vs. DBC and F on PC2. In the latter case, removing the size effect altered the overall relationship patterns.

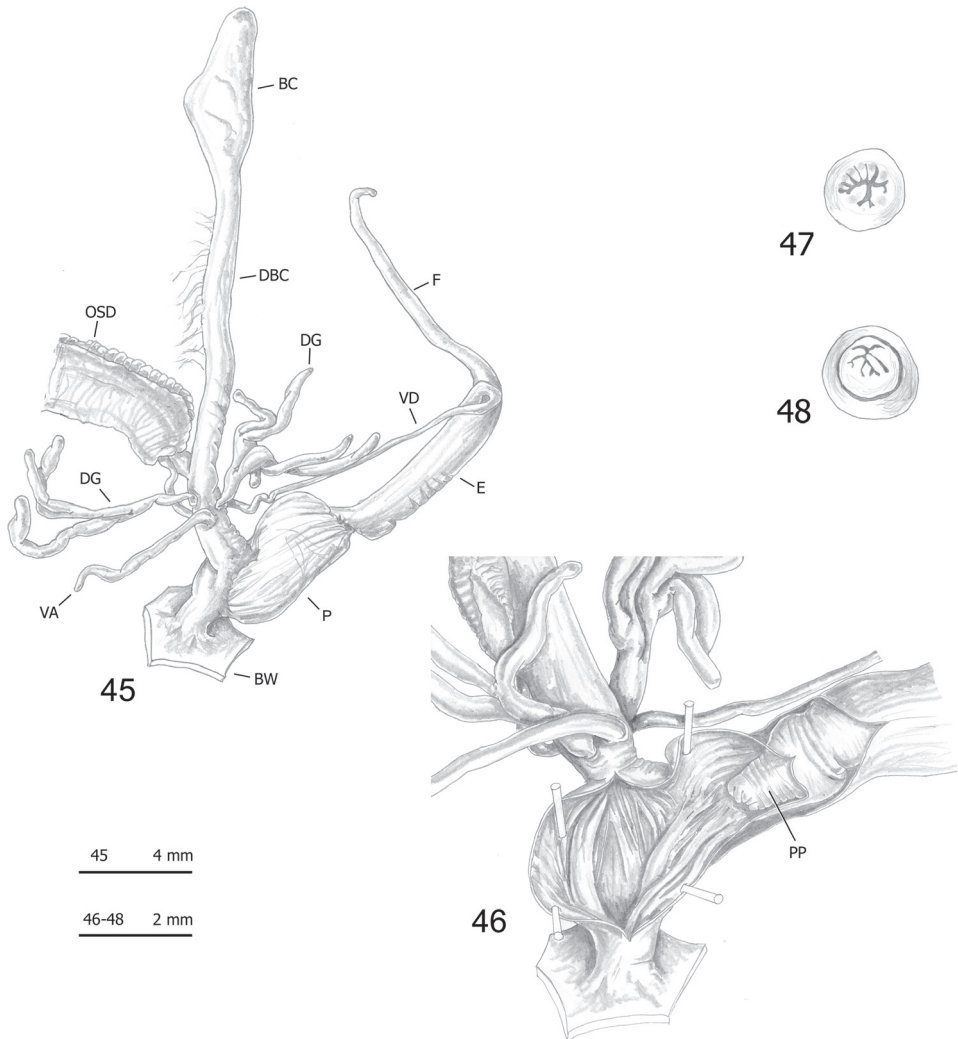


Figures 37–40. Genitalia (proximal parts excluded) (37), internal structure of distal genitalia (38), transverse sections of medial epiphallus (39) and apical penial papilla (40) of *Monacha pantanellii* from Monte Fionchi summit [Fio1] (FGC 8140).



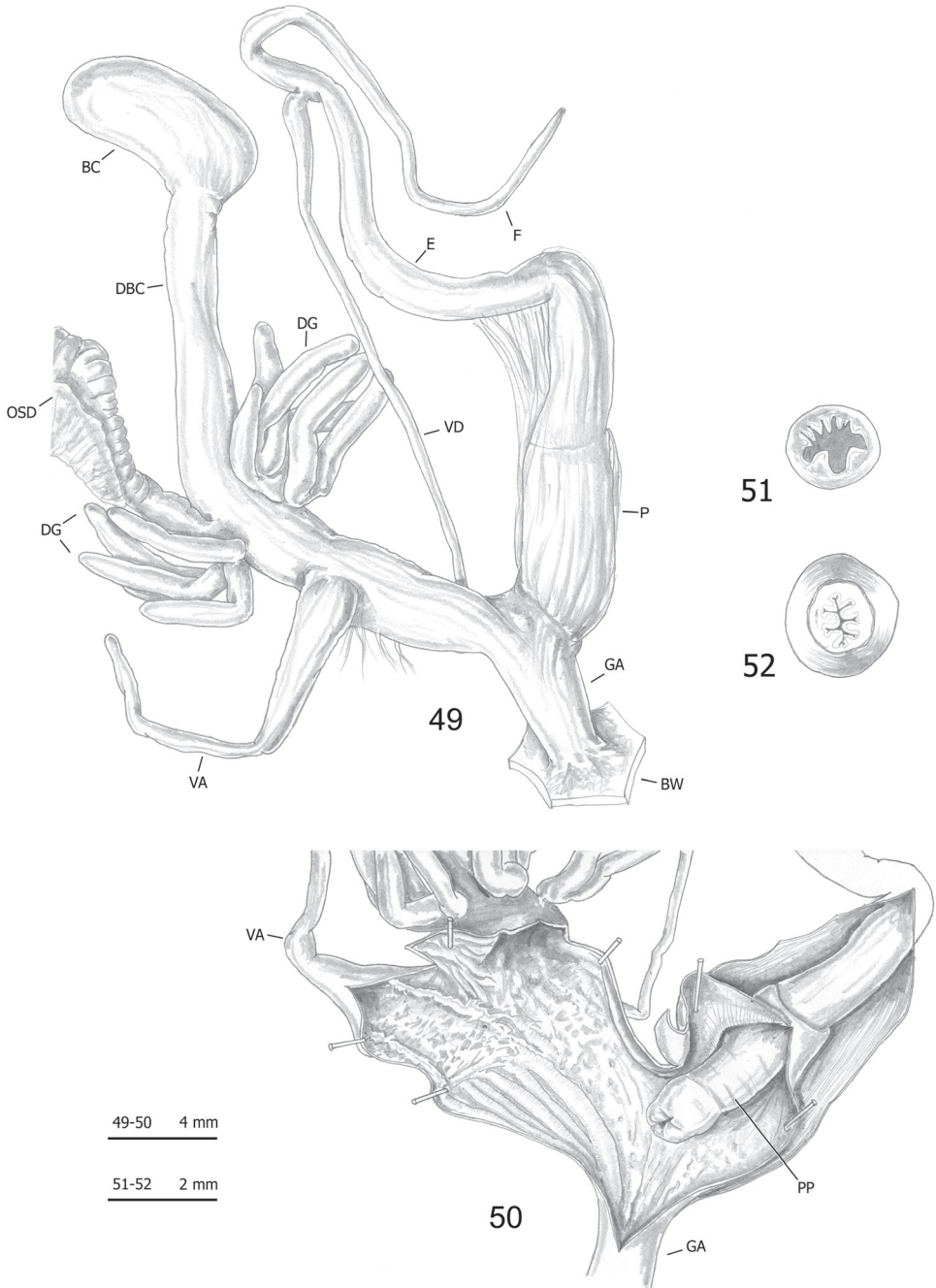
Figures 41–44. Genitalia (proximal parts excluded) (**41**), internal structure of distal genitalia (**42**), transverse sections of medial epiphallus (**43**) and apical penial papilla (**44**) of *Monacha pantanellii* from Monte Fionchi, Torrecola [Fio2] (FGC 38944).

Box plots (Fig. 66) for anatomical characters showed that VA, F and P have the best discriminating value in distinguishing PAN: they distinguished 6 (VA) and 5 (F and P) species or molecular lineage pairs, respectively, according to Dunn's test with Benjamini-Hochberg adjustment ($\alpha = 0.01$), followed by E and V with four and three species or molecular lineage pairs, respectively (Table 6). The most recognisable pairs were PAN vs. CAR and PAN vs. CAN-1 (four significant characters), PAN vs. CAN-2, PAN vs. CAN-3, PAN vs. CAN-5 and PAN vs. PAR (3 significant characters). Only two characters significantly distinguished PAN vs. CAN-4 and only one PAN vs. CAN-6 (Table 6). Anatomical characters have high discriminating value as testified by very low p values after Dunn's test: in most cases (19 of 22) $P < 0.001$ (Table 6).

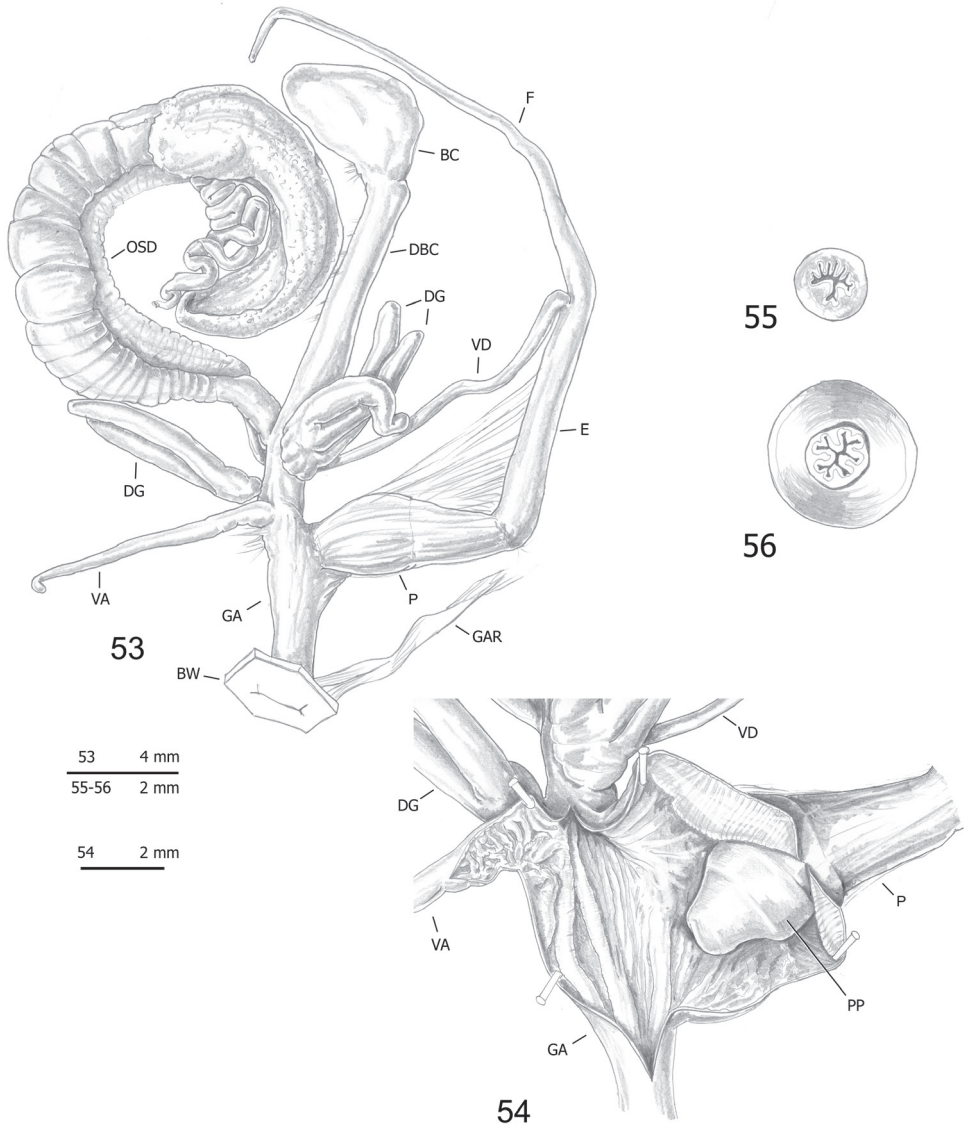


Figures 45–48. Genitalia (proximal parts excluded) (45), internal structure of distal genitalia (46), transverse sections of medial epiphallus (47) and apical penial papilla (48) of *Monacha pantanellii* from Vallonina [Val] (FGC 25345).

RDA with population constraint on the shape and size matrix (Fig. 67) showed that RDA 1 (64%, $P < 0.001$) separated populations Carsoli [Car], Monte Fionchi, Torrecola [Fio2], Turania [Tur1] and Vallonina [Val] from populations Via Salaria, Ornaro Alto [Alt], Valle dell’Aniene [Ani], Via Salaria, Poggio San Lorenzo [Lor] and Lago del Turano [Tur2], with Monte Fionchi, summit [Fio1] and Montero Sabino [Sab] in intermediate position. The preliminary classic PCA revealed size as the first major source of morphological variation, since PC1 (65%) was a positive combination of all variables. On the contrary, RDA 2 (13%, $P < 0.001$) separated population Val



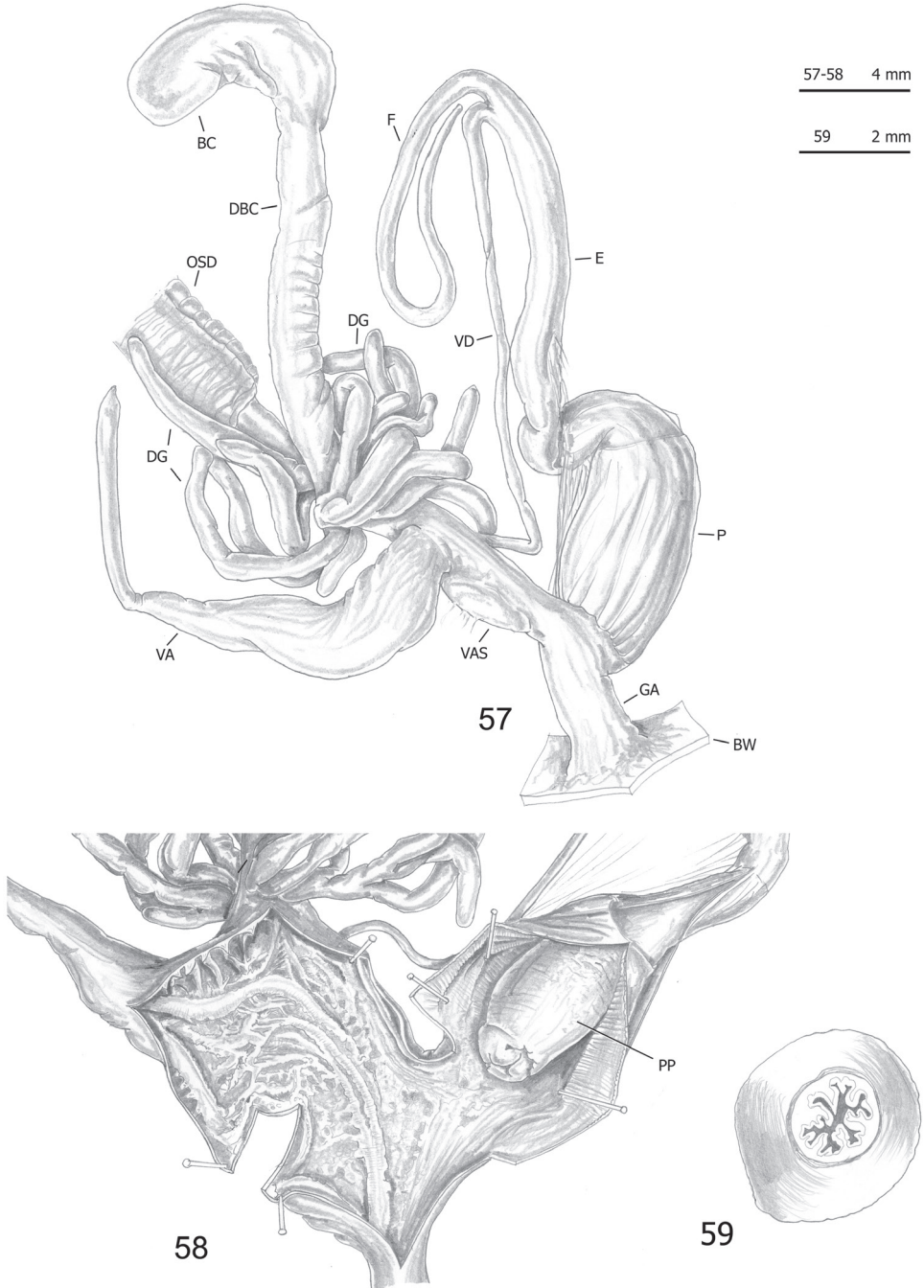
Figures 49–52. Genitalia (proximal parts excluded) (49), internal structure of distal genitalia (50), transverse sections of medial epiphallus (51) and apical penial papilla (52) of *Monacha pantanellii* from Valle dell’Aniene, Roccagiovine [Ani] (FGC 42974).



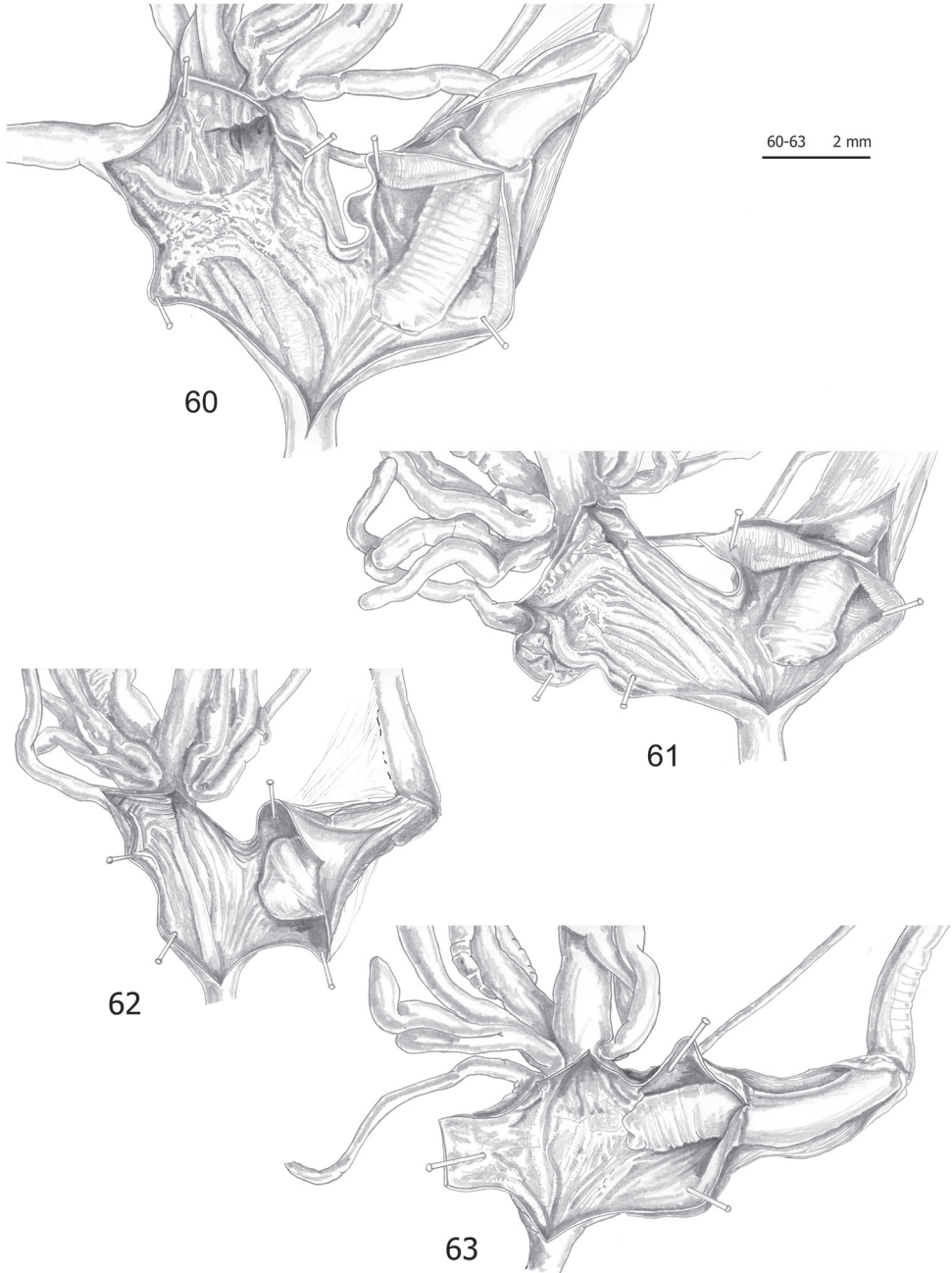
Figures 53–56. Genitalia (proximal parts excluded) (**53**), internal structure of distal genitalia (**54**), transverse sections of medial epiphallus (**55**) and apical penial papilla (**56**) of *Monacha pantanellii* from Carsoli [Car] (FGC 41651).

from populations Sab and Fio1, with all the other populations (Car, Fio2, Tur1, Alt, Ani, Lor and Tur2) in intermediate position. In that regard, PC2 (16.5%) accounted for a contrast between V and VA vs. F and DBC.

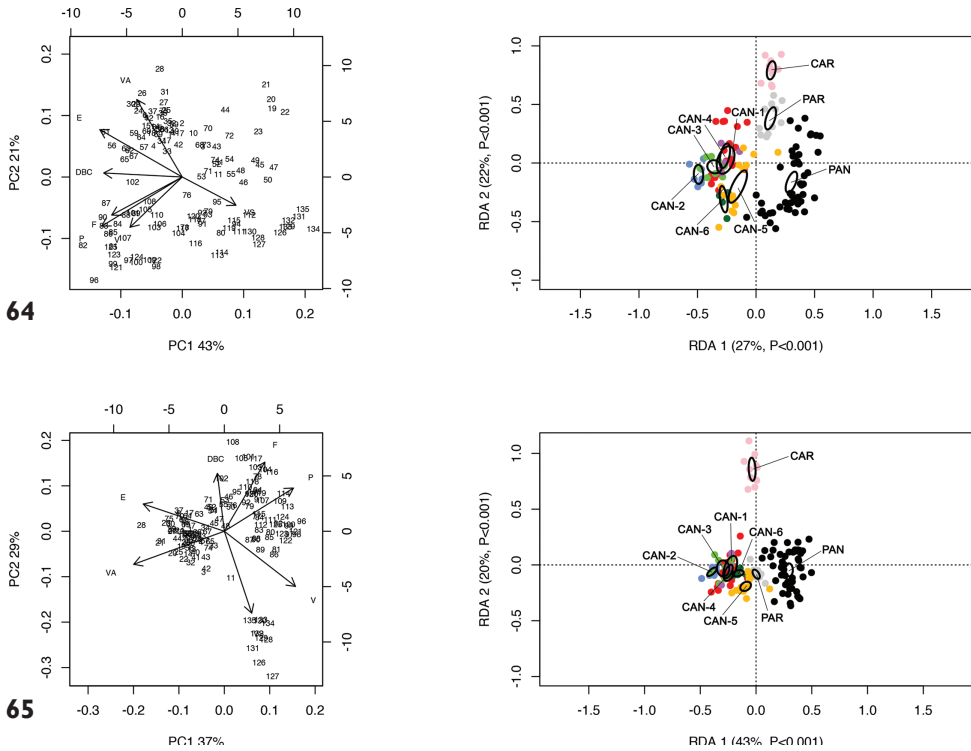
RDA on the shape (Z) matrix (Fig. 68) showed a less clear separation between populations. RDA 1 (43%, $P < 0.001$) separated the population Sab from the group of populations Tur2, Val, Alt and Lor, with Ani, Fio1, Fio2 and Car in intermediate



Figures 57–59. Genitalia (proximal parts excluded) (**57**), internal structure of distal genitalia (**58**) and transverse section of apical penial papilla (**59**) of *Monacha pantanellii* from Lago del Turano [Tur2] (FGC 41654).



Figures 60–63. Internal structure of distal genitalia of *Monacha pantanellii* from Valle dell’Aniene, Roccagiovine [Ani] (FGC 42974) (**60**), Via Salaria, Ornaro Alto [Alt] (FGC 41553) (**61**), Turania [Tur1] (FGC 42971) (**62**) and road to Montenero Sabino [Sab] (FGC 41552) (**63**).



Figures 64, 65. Principal component analysis (PCA) and Redundancy analysis (RDA) with species or molecular lineage constraint applied to the original genital matrix (64) and shape-related Z-matrix (65).

position. Shape-related PCA indicated that V vs. F were the two principal shape determinants on PC1 (39.5%). RDA 2 (14%, P < 0.001) separated Tur2 from Alt, Lor and Fio1, with all the other populations in a more or less intermediate position. In that regard, PC2 (24.5%) accounted for a contrast between PD and VA.

Discussion

Molecular analysis of nucleotide sequences obtained from specimens originating from ten populations occurring in the grasslands of the central Apennines suggests that these populations represent a different species from other Italian *M. cantiana* s. l. lineages (CAN-1, CAN-2, CAN-3, CAN-5, CAN-6) and *Monacha* species (*M. cartusiana* and *M. parumcincta*), populations of which were previously subject to molecular analysis (Pieńkowska et al. 2018a, 2019a, 2019b). In each of the phylogenetic trees, i.e., ML of concatenated sequences for mitochondrial COI+16S rDNA (Fig. 2) and nuclear ITS2+H3 (Fig. 3) gene fragments as well as the BI tree of concatenated sequences COI+16S rDNA+ITS2+H3 (Fig. 4), sequences from these ten populations created

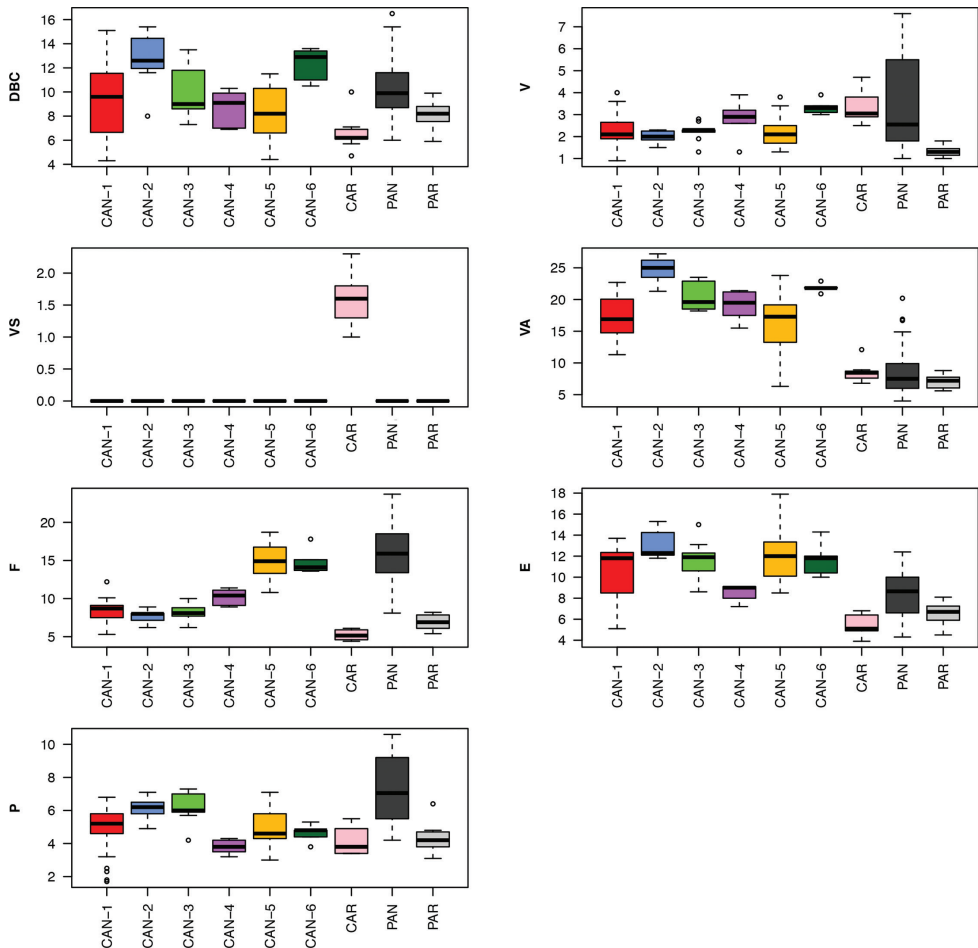
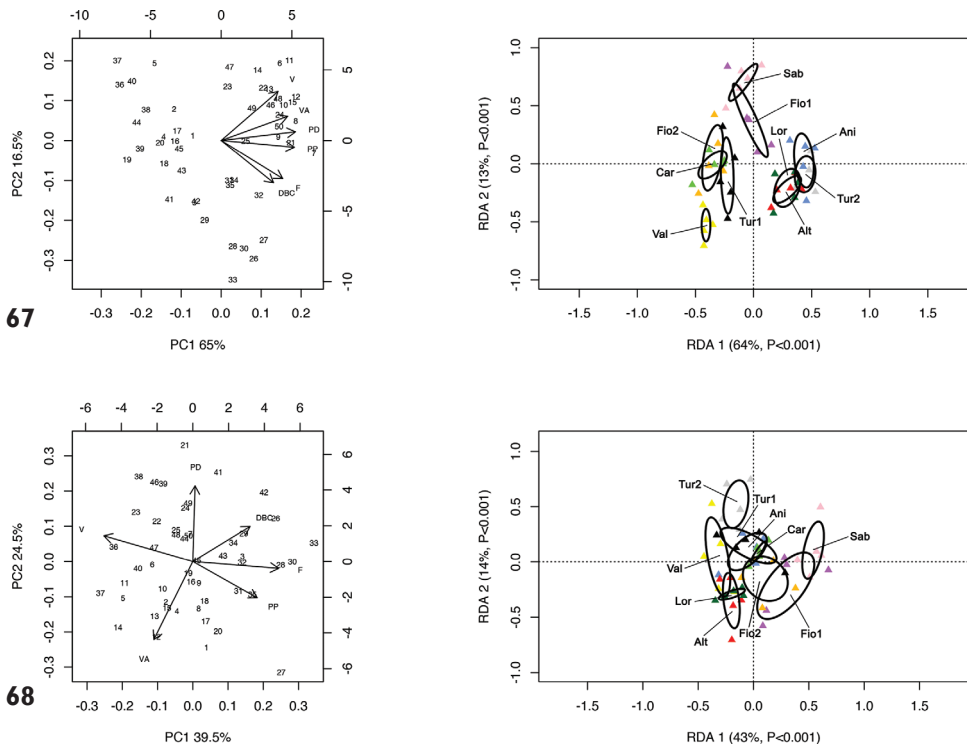


Figure 66. Box plots for genital characters of the ten *Monacha* species or molecular lineages investigated. The lower and upper limits of the rectangular boxes indicate the 25th to 75th percentile range, and the horizontal line within the boxes is the median (50th percentile).

well separated monophyletic clades. Two of these populations represent species described in the past: Monte Fionchi, Summit [Fio1]: *Helix pantanellii* De Stefani, 1879; Vallonina [Val]: *Monacha ruffoi* Giusti, 1973. Molecular analysis confirmed the validity of the species described by Giusti (1973) from the Reatini Mountains, although an older discarded name, introduced by De Stefani (1879), turned out to be available for it.

The range of K2P genetic distances between COI sequences obtained from the ten populations of *M. pantanellii* was 0.2–6.7% (Table 5). We previously found a similar range of K2P distances within populations of *M. cantiana* s. l. CAN-1/CAN-2 (0.2–5.3%; Pieńkowska et al. 2018a, 2019b), *M. cartusiana* (0.0–3.3%; Pieńkowska et al. 2015, 2016, 2018b), *M. parumcincta* (0.2–4.6%; Pieńkowska et al.



Figures 67, 68. Principal component analysis (PCA) and Redundancy analysis (RDA) with population constraint applied to the original genital matrix (**67**) and shape-related Z-matrix (**68**) of specimens of *Monacha pantanellii*.

2018a, 2019b) and *M. claustralis* (0.0–5.7%; Pieńkowska et al. 2015, 2016, 2018b). It is worth noting that this K2P distance range was even narrower (0.2–4.5%) if we considered all but three of 53 the COI sequences obtained from *M. pantanellii* specimens. The three COI sequences excluded were found in single (one or two) specimens of populations from Carsoli [Car], Valle del Turano [Tur1] and Vallonina [Val], however COI sequences obtained from the other specimens of these populations were more similar to others found in *M. pantanellii*. This suggests higher intra-population variation within these three populations, which may prove speciation seen in a rapidly evolving mitochondrial genome (Thomaz et al. 1996; Remigio and Hebert 2003).

The conclusion that ten populations from the central Apennines form a different species is supported by the analysis of K2P genetic distances of COI sequences (Table 5). Although the utility of the 3% barcode threshold as a marker for species distinction, applied in the so-called “barcode method” based on COI sequences (Hebert et al. 2003a, 2003b, 2018; Pentinsaari et al. 2020), is disputable (Davison et al. 2009; Sauer and Hausdorf 2010, 2012; Köhler and Johnson 2012; Batomalaque et al.

2019; Koch et al. 2020), COI sequences have been used to analyse taxonomic problems in different gastropod families (e.g., Remigio and Hebert 2003; Elejalde et al. 2008; Duda et al. 2011; Breugelmans et al. 2013; Proćków et al. 2013, 2019; Čandek and Kuntner 2015; Walther et al. 2016; Kruckenhauser et al. 2017; Galan et al. 2018; Gladstone et al. 2019; Harl et al. 2019; Kneubühler et al. 2019; Bamberger et al. 2020). They were also useful in our previous studies on *Monacha* species (Pieńkowska et al. 2015, 2018a, 2019a, 2019b). Indeed, we have always emphasised that phylogenetic analysis cannot be based on a single gene locus but should combine several mitochondrial and nuclear genes (Pieńkowska et al. 2015, 2018a, 2019a, 2019b). Note that the conclusion that ten populations are distinct from other *Monacha* species at species level is not only supported by the analysis of COI sequences, but also of 16S rDNA, ITS2, and H3.

Moreover, we have always stressed (Pieńkowska et al. 2015, 2018a, 2019a, 2019b) that molecular features alone are insufficient to define species but need to be supported by morphological (shell and anatomy) features. Inconsistency between molecular and morphological features may occur among snail populations or species (Cameron 1992; Cameron et al. 1996; Sauer and Hausdorf 2012; Falniowski et al. 2020), because according to the concept of morphostatic evolution (Gittenberger 1991; Davis 1992; Koch et al. 2020) speciation may be reflected earlier in molecular than in morphological features.

It is not possible to distinguish *M. pantanellii* from the lineages of the *M. cantiana* group on the basis of shell characters, perhaps with the exception of CAN-6 (see Figs 32–34; Table 6). However, this may be biased by the fact that only one population of this lineage was available for study (Pieńkowska et al. 2019b). With regard to the other two species examined by comparison, *M. cartusiana* and *M. parumcincta*, the analysis found that distinguishing *M. pantanellii* from the former is difficult (only two characters have discriminating value), but from the latter is easy (eight characters have discriminating value). Anyway, these species are readily distinguished by colour pattern. *M. cartusiana* has a smoother more glossy shell, usually whitish, often with sharp milky-white subsutural and peripheral bands, intensely reddish-brown peristome, externally bordered by a ring of bright milky white. *M. parumcincta* has a shell similar to that of *M. pantanellii*, but less glossy and more opaque, sometimes with paler peripheral and subsutural bands and brownish peristome, externally bordered by a pale whitish ring.

The distinction of *M. pantanellii* based on anatomical characters is clear from the lineages of the *M. cantiana* group and the other two species examined by comparison, *M. cartusiana* and *M. parumcincta*. However, contrary to the situation with shell characters, CAN-6 is the lineage least distinct from *M. pantanellii*: again, the few specimens available may have biased the result. The analysis confirmed the high discriminating value of the vaginal appendix which distinguishes *M. pantanellii* from all the lineages of the *M. cantiana* group and *M. cartusiana*. The penis and flagellum are also important because they significantly distinguish *M. pantanellii* from five other species or molecular lineages (Table 6).

Table 7. Other anatomical features distinguishing *Monacha* species.

Characters	<i>M. pantanellii</i>	<i>M. cantiana</i> group	<i>M. cartusiana</i>	<i>M. parumcincta</i>
insertion of VA	vaginal	atrial	vaginal	atrial
shape of VA	usually short and slender, calibre almost constant; however, in two populations it is long or very long with proximal portion (ca. half its length or more) very enlarged and distal portion slender	long or very long, not slender nor enlarged, calibre initially large then progressively tapered; sometimes with variably evident basal sac	long or very long with proximal portion (ca. half its length or less) enlarged and distal portion slender	usually short and enlarged, calibre almost constant
PP	with thick external walls and narrow space between external walls and central duct; central duct circular in transverse section, usually rather small in diameter, not joined by strips to external walls and with its lumen almost totally filled by large pleats	with thick external walls, and narrow to wide space between external walls and central duct; central duct circular in transverse section, usually rather large in diameter, joined by strips to external walls and with its lumen not filled by large pleats	with thick external walls and narrow to wide space between external walls and circular central duct; central duct circular in transverse section, usually medium-sized in diameter, not joined by strips to external walls and with its lumen almost totally filled by large pleats	with thin external walls and narrow space between external walls and central duct; central duct horseshoe-shaped in transverse section, large in diameter, not joined by strips to external walls and with its lumen apparently not filled by pleats
References	Giusti (1973: figs 26A, B), this paper (Figs 38–64)	Pieńkowska et al. (2018a: figs 20–50; 2019a: figs 2–3; 2019b: figs 19–41)	Giusti and Manganello (1987: figs 1A–G), Pieńkowska et al. (2015: figs 11–12, 15–16, 18–21)	Pieńkowska et al. (2018a: figs 51–59)

Other anatomical features that distinguish *M. pantanellii* from the *M. cantiana* group, *M. cartusiana* and *M. parumcincta* were not included in the analysis, since it is impossible to quantify them. They are the insertion of the vaginal appendix, the shape of the vaginal appendix, and the section of the penial papilla (Table 7).

Intraspecific variability in *M. pantanellii* is high and concerns both shell and genitalia. Inter-population shell variability mainly affects the size features: some populations are distinguished by reduced size, notably the one from Carsoli [Car] (Figs 30, 31) and the slightly larger populations from Turania [Tur1] (Figs 11–14) and Vallonina [Val] (Figs 21, 22). This pattern was confirmed by RDA on the original shell matrix (Fig. 32) and by its disappearance when the size effect was removed (Fig. 33). Anatomically, these populations agree very well with the characters typical of the species (e.g., VA, PD, F) suggesting that shell size has no phylogenetic signal and cannot be used to support taxonomic distinctions. We can hypothesize that it depends on local conditions of drought, food availability and lack of refuges.

Intra-population shell variability is smaller, but the variation of UD from Via Salaria, Ornaro Alto [Alt] is notable (0.9–2.4 mm) including almost the extremes of the range (Figs 18–20).

Inter-population genital variability is more intricate although the size effect is again evident: RDA 1 (Fig. 35) separates the populations of smaller size, i.e., those from Car-

soli [Car], Monte Fionchi, Torrecola [Fio2], Turania [Tur1] and Vallonina [Val], from those of larger size, namely Via Salaria, Ornaro Alto [Alt], Valle dell'Aniene, Roccagiovine [Ani], Via Salaria, Poggio San Lorenzo (Lor) and Lago del Turano [Tur2]. When the size effect is removed (Fig. 36) some patterns persist, albeit less clear because conflicting variables are involved. Inter-population genital variability concerns all anatomical sections but is higher in V and VA (as shown by PCA). The former (V) is very short in Montenero Sabino [Sab] (Fig. 63), Monte Fionchi, Torrecola [Fio2] (Fig. 41) and Carsoli [Car] populations (Fig. 53) and long in those from Via Salaria, Ornaro Alto [Alt] (Fig. 61), Via Salaria, Poggio San Lorenzo [Lor] (not shown), Valle dell'Aniene, Roccagiovine [Ani] (Fig. 49) and Lago del Turano [Tur2] (Fig. 57). The latter (VA) is usually short but is long in Valle dell'Aniene, Roccagiovine [Ani] (Fig. 49) and very long in Lago del Turano [Tur2] populations (Fig. 57), where however intra-population range is wide.

According to RDA on the shape (Z) matrix, some of the most divergent populations are those from Montenero Sabino [Sab] and Lago del Turano [Tur2], which fall at the extremes of the ordination figure (Fig. 68).

This revision is the first result of research on the *Monacha* species living in the mountain grasslands of the central Apennines. It confirms the validity of the species described by Giusti (1973) from the Reatini Mountains, though an older discarded name, introduced by De Stefani (1879), turned out to be available for it.

It is evident from the above discussion that the species of *Monacha* and the lineages of *M. cantiana* s. l. can only occasionally be recognised morphologically and are also subject to significant inter- and intra-population variability. In this situation, revision based on type material consisting of shells may be not decisive. We therefore took an overall approach that considers shell, genital and molecular evidence to establish a reliable taxonomic setting. Only a multidisciplinary investigation of populations from the type locality, matching type specimens, can clarify the identity of old established *Monacha* taxa. This what we tried to do, although it was made difficult by the fact that the type locality was not always reported in a detailed way. Luckily this was not the case of the species described by De Stefani (1879). Thus, the investigation of specimens from the type locality, the summit of Monte Fionchi near Spoleto in Umbria, enabled us to ascertain that they have the same anatomical features as *M. ruffoi*. Conspecificity of the topotypical populations of *M. pantanellii* and *M. ruffoi* is also strongly supported by molecular analysis. Consequently, the latter has to be regarded as a junior synonym of De Stefani's species.

Since *M. pantanellii* is a *Monacha* species with distinctive anatomical features, we checked all the material accessible to us. This enabled us to find other populations of the species, some from the Reatini Mountains, where they were collected by one of us in the 1960s during field work, some from other more northern mountain ranges (Table 3).

Regarding relationships of *M. pantanellii* with other taxa described or reported from the central Apennines, research is underway. So far we can only reveal that they belong to lineages different from this species and the *M. cantiana* group.

Redescription of *Monacha pantanellii* (De Stefani, 1879)

Monacha pantanellii (De Stefani, 1879)

Figures 5–31, 37–63

Helix pantanellii De Stefani, 1879: 40–41.

Monacha ruffoi Giusti, 1973: 533–537, pl. 6.

Diagnosis. A species of *Monacha* (s. str.) (according to the subgeneric division proposed by Neiber and Hausdorf 2017) with vaginal appendix usually short and slender (having shape and size of a digitiform gland) inserted at mid vagina; proximal vaginal sac absent; penial flagellum long to very long; penial papilla with narrow space between external walls and central duct; central duct circular in transverse section, usually rather small in diameter, not joined by strips to external walls and with its lumen almost totally filled by large pleats.

Redescription. *Shell* (Figs 5–31) dextral, sub-globose to globose, small to medium in size, variable in colour, sometimes (when colour is brownish yellow) with paler sub-sutural and peripheral bands, with 5¼–6 slightly convex whorls separated by superficial sutures; aperture slightly prosocline, round to oval; peristome not reflected, thickened, with variably evident whitish callous rim lining the outer margin; umbilicus open, very small to small; protoconch and teleoconch smooth, with very faint scattered collabral growth lines. Shell dimensions: H: 10.3 ± 1.5 mm; D: 16.2 ± 2.3 mm (n = 45).

Radula not examined.

Female distal genitalia (Figs 37, 38, 41, 42, 45, 46, 49, 50, 53, 54, 57, 58, 60–63; Table 7) include free oviduct, bursa copulatrix and its duct, digitiform glands, vagina and vaginal appendix. Free oviduct short and variably wide. Bursa copulatrix bean-like or pyriform with long wide duct. Vagina short to long and wide. Digitiform glands disposed on opposite sides of vagina in two groups of 1–3 tufts, each with 1–3 units. Vaginal appendix usually short (having shape and size of a digitiform gland) and inserted approximately half-way along the vagina.

Male distal genitalia (Figs 37–63, Table 7) include vas deferens, flagellum, epiphallus and penis. Vas deferens very long and very slender. Flagellum long to very long and slender. Epiphallus long to very long and wide. Penis short and wide, enveloped by thin sheath, consisting of proximal portion (from start of penial sheath to base of penial papilla) and distal portion (from base of penial papilla to genital atrium). Penial papilla variable in shape (perhaps due to pre-mortem stress or spirit fixation), with apical opening, thick external walls and narrow space between external walls and central duct; central duct circular in section, usually rather small in diameter, not joined by strips to external walls of penial papilla and with its lumen almost totally filled with large pleats.

Genital atrium large, receiving vagina and penis, internally smooth or with variably developed longitudinal pleats.

Type locality. “Sulla cima del Monte Fionghi al sud di Spoleto a circa mille metri sul livello del mare”, i.e., on the summit of Monte Fionchi, south of Spoleto, at an altitude of ca. 1000 m (municipality of Spoleto, province of Perugia), UTM references 32T UH 1726, Lat and Long: 42°40.455'N, 12°46.340'E.

Type material. Probably lost.

Topotype sequences. Sequences obtained from individuals from the type locality of *M. pantanellii* are designated as typical for this species: COI – MT380011–MT380018, 16S rDNA – MT376031–MT376039, ITS2 – MT376088–MT376094, H3 – MT385776–MT385785.

Etymology. Named after Dante Pantanelli (1844–1913), Italian palaeontologist and geologist at the University of Modena. He published many papers on Miocene and Pliocene molluscs, some of which were co-authored by his friend Carlo De Stefani (1851–1924). He was also the secretary of the Italian Malacological Society and the editor of the *Bullettino della Società Malacologica Italiana* for many years (Manganelli et al. 2017, with references).

Giusti's species was named after Sandro Ruffo (1915–2010), a major Italian twentieth-century zoologist and director of the Museo Civico di Storia Naturale di Verona for many years (Latella 2011).

Distribution. Endemic to Umbria-Marche Apennines and Latium Sub-Apennines. It occurs from the Apennines of Gualdo Tadino in the north to the Aniene and Turano valleys in the south.

Ecology. Mesophile species living among grass in open habitats such as grasslands, pastures, forest edges and clearings in hill and mountain areas.

Conservation. Apparently common and widespread species within its range, but in some sites (e.g., Vallonina) it was no longer found during a field survey in the summer of 2019. Like other mesophilic species it could be sensitive to global warming.

Remarks. This species was distinguished from *Monacha cantiana* on the basis of a few shell characters (“more depressed, more fragile and paler shell, with fine growth lines, less rounded opening and deeper umbilicus”) and was disregarded by its author as an “extreme variety” of the former. Subsequently it was only reported in two catalogues by Westerlund (1889: 95) and Pilsbry (1895: 266) so that when Alzona prepared the catalogue of Italian non-marine malacofauna, they included it as a doubtful species (Alzona 1971: 183).

On the contrary, our analysis showed that it matches a valid species, currently known as *Monacha ruffoi*, described from the Reatini mountains by Giusti (1973) as a *Monacha* species with a shell resembling that of *cantiana*, but with a much smaller vaginal appendix.

This is an unexpected result: indeed, De Stefani's species is one of thousands of mollusc species established since the second half of the nineteenth century on the basis of very few shell features of no diagnostic value due to dramatic intra- and inter-population variability. In describing thousands of species and varieties, past authors hit on some that remained valid.

Acknowledgements

We thank Helen Ampt (Siena, Italy) for revising the English, Giovanni Cappelli (Siena, Italy) for taking photographs of the shells, Jarosław Bogucki (Poznań, Poland) for drawing a map (Fig. 1), Alexis Dunno (Portland State University, USA) for precious statistical advice about the use of the R package “dunn.test”. We are very grateful to Bernhard Hausdorf (University of Hamburg, Germany) and to Eike Neubert (Naturhistorisches Museum, Bern, Switzerland) for their valuable comments on the manuscript.

References

- Alzona C (1971) Malacofauna italiana. Catalogo e bibliografia dei Molluschi viventi, terrestri e d’acqua dolce. Atti della Società Italiana di Scienze Naturali e del Museo Civico di Storia Naturale di Milano 111: 1–433.
- Bamberger S, Duda M, Tribsch A, Haring E, Sattmann H, Macek O, Affenzeller M, Kruckenhauer L (2020) Genome-wide nuclear data confirm two species in the Alpine endemic land snail *Noricella oreinos* s.l. (Gastropoda, Hygromiidae). Journal of Zoological Systematics and Evolutionary Research 00: 1–23. <https://doi.org/10.1111/jzs.12362>
- Batomaque GA, Que GCL, Itong TAB, Masanga ARL, Chavez ERC de, Fontanilla IKC (2019) Cytochrome c oxidase subunit 1 (COI) profile of the Philippine Helicostylinae (Gastropoda: Stylommatophora: Camaenidae). Philippine Journal of Science (Special Issue on Genomics) 148: 1–13.
- BioEdit (2017) BioEdit 7.2 <https://bioedit.software.informer.com/7.2>
- Bruegelmans K, Jordaens K, Adriaens E, Remon JP, Cardona JQ, Backeljau T (2013) DNA barcodes and phylogenetic affinities of the terrestrial slugs *Arion gilvus* and *A. ponsi* (Gastropoda, Pulmonata, Arionidae). ZooKeys 365: 83–104. <https://doi.org/10.3897/zookeys.365.6104>
- Cameron RAD (1992) Land snail faunas of the Napier and Oscar ranges, Western Australia: diversity, distribution and speciation. Biological Journal of the Linnean Society 45: 271–286. <https://doi.org/10.1111/j.1095-8312.1992.tb00644.x>
- Cameron RAD, Cook LM, Hallows JD (1996) Land snails on Porto-Santo: adaptive and non-adaptive radiation. Philosophical Transactions of the Royal Society of London B 351: 309–327. <https://doi.org/10.1098/rstb.1996.0025>
- Čandek K, Kuntner M (2015) DNA barcoding gap: reliable species identification over morphological and geographical scales. Molecular Ecology Resources 15: 268–277. <https://doi.org/10.1111/1755-0998.12304>
- Davis GM (1992) Evolution of prosobranch snails transmitting Asian *Schistosoma*: coevolution with *Schistosoma*: a review. Progress in Clinical Parasitology 3: 145–204. https://doi.org/10.1007/978-1-4612-2732-8_6
- Davison A, Blackie RL, Scothern GP (2009) DNA barcoding of stylommatophoran land snail: a test of existing sequences. Molecular Ecology Resources 9: 1092–1101. <https://doi.org/10.1111/j.1755-0998.2009.02559.x>

- De Stefani C (1879) Nuove specie di molluschi viventi nell'Italia centrale. *Bullettino della Società Malacologica Italiana* 5(1/3): 38–48. <https://www.biodiversitylibrary.org/page/38908268>
- Dinno A (2017) dunn.test: Dunn's Test of Multiple Comparisons Using Rank Sums. R package version 1.3.5. <https://CRAN.R-project.org/package=dunn.test>
- Duda M, Sattmann H, Haring E, Bartel D, Winkler H, Harl J, Kruckenhauser L (2011) Genetic differentiation and shell morphology of *Trochulus oreinos* (Wagner, 1915) and *T. hispidus* (Linnaeus, 1758) (Pulmonata: Hygromiidae) in the northeastern Alps. *Journal of Molluscan Studies* 77: 30–40. <https://doi.org/10.1093/mollus/eyq037>
- Elejalde MA, Madeira MJ, Muñoz B, Arrébola JR, Gómez-Moliner BJ (2008) Mitochondrial DNA diversity and taxa delineation in the land snails of the *Iberus gualterianus* (Pulmonata, Helicidae) complex. *Zoological Journal of the Linnean Society* 154: 722–737. <https://doi.org/10.1111/j.1096-3642.2008.00427.x>
- Falniowski A, Heller J, Cameron RAD, Pokryszko BM, Osikowski A, Rysiewska A, Hofman S (2020) Melanopsidae (Caenogastropoda: Cerithioidea) from the eastern Mediterranean: another case of morphostatic speciation. *Zoological Journal of Linnean Society* 190: 483–507. <https://doi.org/10.1093/zoolinnean/zlz160>
- Felsenstein J (1985) Confidence limits on phylogenies: an approach using the bootstrap. *Evolution* 39: 783–791. <https://doi.org/10.1111/j.1558-5646.1985.tb00420.x>
- Fiorentino V, Manganelli G, Giusti F, Ketmaier V (2016) Recent expansion and relic survival: Phylogeography of the land snail genus *Helix* (Mollusca, Gastropoda) from south to north Europe. *Molecular Phylogenetics and Evolution* 98: 358–372. <https://doi.org/10.1016/j.ympev.2016.02.017>
- Fiorentino V, Salomone N, Manganelli G, Giusti F (2010) Historical biogeography of Tyrrhenian land snails: the *Marmorana*–*Tyrrheniberus* radiation (Pulmonata, Helicidae). *Molecular Phylogenetics and Evolution* 55: 26–37. <https://doi.org/10.1016/j.ympev.2009.11.024>
- Fitzinger LI (1833) Systematisches Verzeichniß der im Erzherzogthume Oesterreich vorkommenden Weichthiere, als Prodrum einer Fauna derselben. Beiträge zur Landeskunde Oesterreich's unter der Enns 3: 88–122. Wien. <https://doi.org/10.5962/bhl.title.10037>
- Forcart L (1965) Rezente Land-und Süßwassermollusken der süditalienischen Landschaften Apulien, Basilicata und Calabrien. *Verhandlungen der Naturforschenden Gesellschaft in Basel* 76: 59–184.
- Galan GL, Mendez NP, Dela Cruz RY (2018) DNA barcoding of three selected gastropod species using cytochrome oxidase (COI) gene. *Annals of West University of Timișoara, series Biology* 21: 93–102.
- Gladstone NS, Niemiller ML, Pieper EB, Dooley KE, McKinney ML (2019) Morphometrics and phylogeography of the cave-obligate land snail *Helicodiscus barri* (Gastropoda, Stylommatophora, Helicodiscidae). *Subterranean Biology* 30: 1–30. <https://doi.org/10.3897/subtbiol.30.35321>
- Glez-Peña D, Gómez-Blanco D, Reboiro-Jato M, Fdez-Riverola F, Posada D (2010) ALTER: program-oriented format conversion of DNA and protein alignments. *Nucleic Acids Research* 38 (Web Server issue): W14–W18. <https://doi.org/10.1093/nar/gkq321>

- Gittenberger E (1991) What about non-adaptive radiation? *Biological Journal of the Linnean Society* 43: 263–272. <https://doi.org/10.1111/j.1095-8312.1991.tb00598.x>
- Giusti F (1973) Notulae malacologicae XVI. I molluschi terrestri e di acqua dolce viventi sul massiccio dei Monti Reatini (Appennino Centrale). *Lavori della Società Italiana di Biogeografia (Nuova Serie)* 2 [“1971”] : 423–574, Tav. I-VII [= 1–7]. Forlì. <https://doi.org/10.21426/B62110484>
- Hall TA (1999) BioEdit: a user friendly biological sequence alignment editor and analysis program for Windows 95/98/NT. *Nucleic Acids Symposium Series* 41: 95–98.
- Harl J, Haring E, Páll-Gergely B (2019) Hybridization and recurrent evolution of left–right reversal in the land snail genus *Schileykula* (Orculidae, Pulmonata). *Journal of Zoological Systematics and Evolutionary Research* 58: 633–647. <https://doi.org/10.1111/jzs.12353>
- Hartmann JDW (1844) *Erd- und Süßwasser-Gasteropoden der Schweiz. Mit Zugabe einiger merkwürdigen exotischen Arten. I. Band.* Scheitlin & Zollikofer, St. Gallen, XX+227+84 pp. <https://doi.org/10.5962/bhl.title.15378>
- Hasegawa M, Kishino H, Yano T (1985) Dating the human-ape split by a molecular clock of mitochondrial DNA. *Journal of Molecular Evolution* 22: 160–174. <https://doi.org/10.1007/BF02101694>
- Hebert PDN, Braukmann TWA, Prosser SWJ, Ratnasingham S, deWaard JR, Ivanova NV, Janzen DH, Hallwachs W, Naik S, Sones JE, Zakharov EV (2018) A Sequel to Sanger: amplicon sequencing that scales. *BMC Genomics* 19: 219. <https://doi.org/10.1186/s12864-018-4611-3>
- Hebert PDN, Cywinska A, Ball SL, deWaard JR (2003a) Biological identifications through DNA barcodes. *Proceedings of the Royal Society B: Biological Sciences* 270: 313–321. <https://doi.org/10.1098/rspb.2002.2218>
- Hebert PDN, Ratnasingham S, deWaard JR (2003b) Barcoding animal life: cytochrome c oxidase subunit I divergences among closely related species. *Proceedings of the Royal Society B: Biological Sciences* 270 (Suppl. 1): 596–599. <https://doi.org/10.1098/rsbl.2003.0025>
- Kimura M (1980) A simple method for estimating evolutionary rate of base substitutions through comparative studies of nucleotide sequences. *Journal of Molecular Evolution* 16: 111–120. <https://doi.org/10.1007/BF01731581>
- Kneubühler J, Hutterer R, Pfarrer B, Neubert E (2019) Anatomical and phylogenetic investigation of the genera *Alabastrina* Kobelt, 1904, *Siretia* Pallary, 1926, and *Otala* Schumacher, 1817 (Stylommatophora, Helicidae). *ZooKeys* 843: 1–37. <https://doi.org/10.3897/zookeys.843.32867>
- Kobelt W (1871) *Catalog der im europäischen Faunengebiet lebenden Binnenconchylien. Mit besonderer Berücksichtigung der in Rossmässler's Sammlung enthaltenen Arten.* T. Fischer, Cassel, 150 pp.
- Koch EL, Neiber MT, Walther F, Hausdorf B (2020) Patterns and processes in a non-adaptive radiation: *Alopi*a (Gastropoda, Clausiliidae) in the Bucegi Mountains. *Zoologica Scripta* 49: 280–294. <https://doi.org/10.1111/zsc.12406>
- Köhler F, Johnson MS (2012) Species limits in molecular phylogenies: a cautionary tale from Australian land snails (Camaenidae: *Amplirhagada* Iredale, 1933). *Zoological Journal of the Linnean Society* 165: 337–362. <https://doi.org/10.1111/j.1096-3642.2011.00810.x>

- Kruckenhauser L, Haring E, Tautscher B, Cadahía L, Zopp L, Duda M, Harl J, Sattmann H, Kirchner S (2017) Indication for selfing in geographically separated populations and evidence for Pleistocene survival within the Alps: the case of *Cylindrus obtusus* (Pulmonata: Helicidae). *BMC Evolutionary Biology* 17: 138. <https://doi.org/10.1186/s12862-017-0977-0>
- Kumar S, Stecher G, Tamura K (2016) MEGA7: Molecular Evolutionary Genetics Analysis version 7.0 for bigger datasets. *Molecular Biology and Evolution* 33: 1870–1874. <https://doi.org/10.1093/molbev/msw054>
- Latella L (ed.) (2011) Sandro Ruffo. Ricordi di allievi e amici. Museo Civico di Storia Naturale di Verona, Verona, 199 pp.
- Linnaeus C (1758) *Systema naturæ per regna tria naturæ, secundum classes, ordines, genera, species, cum characteribus, differentiis, synonymis, locis*. Editio decima, reformata. Tomus I. Salvius, Holmiæ, 4+824 pp. <https://doi.org/10.5962/bhl.title.542>
- Manganelli G, Bodon M, Favilli L, Giusti F (1995) Gastropoda Pulmonata. In: Minelli A, Ruffo S, La Posta S (Eds) Checklist delle specie della fauna d'Italia 16. Calderini, Bologna, 1–60.
- Manganelli G, Lori E, Benocci A, Cianfanelli S (2017) Società Malacologica Italiana 1874–1906. *Archives of Natural History* 44: 303–320. <https://doi.org/10.3366/anh.2017.0451>
- Montagu G (1803) *Testacea Britannica, or, Natural history of British shells, marine, land, and fresh-water, including the most minute: systematically arranged and embellished with figures*. 2 Vols, Romsey, London, 606 pp. <https://doi.org/10.5962/bhl.title.33927>
- Monterosato TA di (1892) Molluschi terrestri delle isole adiacenti alla Sicilia. *Atti della Reale Accademia di Scienze, Lettere e Belle Arti di Palermo* (3) 2: 1–33.
- Müller OF (1774) *Vermium terrestrium et fluviatilium, seu animalium infusorium, helminthicorum, et testaceorum, non marinorum, succincta historia*. Vol. II. Heineck & Faber, Havniae et Lipsiae, 214 pp. <https://doi.org/10.5962/bhl.title.46299>
- Neiber MT, Hausdorf B (2017) Molecular phylogeny and biogeography of the land snail genus *Monacha* (Gastropoda, Hygromiidae). *Zoologica Scripta* 46: 308–321. <https://doi.org/10.1111/zsc.12218>
- Oliverio M, De Matthaeis E, Hallgass A (1993) Genetic divergence between Italian populations of *Marmorana (Ambigua)* (Gastropoda, Pulmonata, Helicidae). *Lavori della Società italiana di Malacologia* 24: 225–248 (1992).
- Pentinsaari M, Ratnasighman S, Miller SE, Hebert PDN (2020) BOLD and GenBank revisited – Do identification errors arise in the lab or in the sequence libraries? *PLoS ONE* 14: e0231814. <https://doi.org/10.1371/journal.pone.0231814>
- Pieńkowska JR, Duda M, Kosicka E, Manganelli G, Giusti F, Lesicki A (2019a) *Monacha cantiana* s.l. (Montagu, 1803) (Gastropoda: Hygromiidae) – mitochondrial lineage occurring in Austria. *Arianta* 7: 33–40.
- Pieńkowska JR, Giusti F, Manganelli G, Lesicki A (2015) *Monacha claustralis* (Rossmässler 1834) new to Polish and Czech malacofauna (Gastropoda: Pulmonata: Hygromiidae). *Journal of Conchology* 42: 79–93. <http://docplayer.net/56112556-Monacha-claustralis-rossmassler-1834-new-to-polish-and-czech-malacofauna-gastropoda-pulmonata-hygromiidae.html>
- Pieńkowska JR, Górka M, Matuszak M, Bocianowski P, Gwardjan M, Lesicki A (2016) New data on distribution and molecular diagnostics of *Monacha claustralis* (Rossmässler, 1834) and *M. cartusiana* (O. F. Müller, 1774) (Gastropoda: Eupulmonata: Hygromiidae) in Po-

- land, Bosnia and Serbia. *Folia Malacologica* 24: 223–237. <https://doi.org/10.12657/fo-mal.024.019>
- Pieńkowska JR, Manganelli G, Giusti F, Barbato D, Hallgass A, Lesicki A (2019b) Exploration of phylogeography of *Monacha cantiana* s.l. continues: the populations of the Apuan Alps (NW Tuscany, Italy) (Eupulmonata, Stylommatophora, Hygromiidae). *ZooKeys* 814: 115–149. <https://doi.org/10.3897/zookeys.814.31583>
- Pieńkowska JR, Manganelli G, Giusti F, Hallgass A, Lesicki A (2018a) Exploring *Monacha cantiana* (Montagu, 1803) phylogeography: cryptic lineages and new insights into the origin of the English populations (Eupulmonata, Stylommatophora, Hygromiidae). *ZooKeys* 765: 1–41. <https://doi.org/10.3897/zookeys.765.24386>
- Pieńkowska JR, Proćków M, Górka M, Lesicki A (2018b) Distribution of *Monacha claustralis* (Rossmässler, 1834) and *M. cartusiana* (O. F. Müller, 1774) (Eupulmonata: Hygromiidae) in central European and Balkan countries: new data. *Folia Malacologica* 26: 103–120. <https://doi.org/10.12657/fo-mal.026.009>
- Pilsbry HA (1895) Helicidae. Guide to the study of helices. In: Tryon GW and Pilsbry HA, Manual of conchology, structural and systematical, with the illustrations of the species. Pulmonata. Second series 9(36): 161–366. [pls 41–71] <https://www.biodiversitylibrary.org/page/23737354>
- Proćków M, Mackiewicz P, Pieńkowska JR (2013) Genetic and morphological studies of species status for poorly known endemic *Trochulus phorochoetius* (Bourguignat, 1864) (Gastropoda: Pulmonata: Hygromiidae), and its comparison with closely related taxa. *Zoological Journal of Linnean Society* 169: 124–143. <https://doi.org/10.1111/zoj.12048>
- Proćków M, Duda M, Kruckenhauser L, Maassen WJM, de Winter AJ, Mackiewicz P (2019) Redescription of the western Balkan species *Xerocampylaea waldemari* and its phylogenetic relationships to other Urticicolini (Gastropoda: Hygromiidae). *Systematics and Biodiversity* 17: 367–384. <https://doi.org/10.1080/14772000.2019.1617365>
- Remigio EA, Hebert PDN (2003) Testing the utility of partial COI sequences for phylogenetic estimates of gastropod relationships. *Molecular Phylogenetics and Evolution* 29: 641–647. [https://doi.org/10.1016/S1055-7903\(03\)00140-4](https://doi.org/10.1016/S1055-7903(03)00140-4)
- Ronquist F, Huelsenbeck JP (2003) MRBAYES 3: Bayesian phylogenetic inference under mixed models. *Bioinformatics* 19: 1572–1574. <https://doi.org/10.1093/bioinformatics/btg180>
- Rossmässler EA (1834) Diagnoses conchyliorum terrestrium et fluviatilium. Zugleich zu Fascikeln natürlicher Exemplare. II Heft. No. 21–40. Arnold, Dresden & Leipzig, 8 pp. <https://doi.org/10.5962/bhl.title.10380>
- Sauer J, Hausdorf B (2010) Reconstructing the evolutionary history of the radiation of the land snail genus *Xerocrassa* on Crete based on mitochondrial sequences and AFLP markers. *BMC Evolutionary Biology* 10: 299. <https://doi.org/10.1186/1471-2148-10-299>
- Sauer J, Hausdorf B (2012) A comparison of DNA-based methods for delimiting species in a Cretan land snail radiation reveals shortcomings of exclusively molecular taxonomy. *Cladistics* 28: 300–316. <https://doi.org/10.1111/j.1096-0031.2011.00382.x>
- Tamura K (1992) Estimation of the number of nucleotide substitutions when there are strong transition-transversion and G + C-content biases. *Molecular Biology and Evolution* 9: 678–687. <https://doi.org/10.1093/oxfordjournals.molbev.a040752>

- Thomaz D, Guiller A, Clarke B (1996) Extreme divergence of mitochondrial DNA within species of pulmonate land snails. *Proceedings of Royal Society B: Biological Sciences* 263: 363–368. <https://doi.org/10.1098/rspb.1996.0056>
- Thompson JD, Higgins DG, Gibson TJ (1994) CLUSTAL W: improving the sensitivity of progressive multiple sequence alignment through sequence weighting, position specific gap penalties and weight matrix choice. *Nucleic Acids Research* 22: 4673–4680. <https://doi.org/10.1093/nar/22.22.4673>
- Villa A, Villa GB (1841) *Dispositio systematica conchyliarum terrestrium et fluviatilium quae adservantur in collectione fratrum Ant. et Jo. Bapt. Villa conspectu abnormitatum novarumque specierum descriptionibus adjectis*. Borroni & Scotti, Mediolani, 62, [2] pp. <https://doi.org/10.5962/bhl.title.137439>
- Walther F, Neiber MT, Hausdorf B (2016) Species complex or complex species? Integrative taxonomy of the land snail genus *Rossmassleria* (Gastropoda, Helicidae) from Morocco and Gibraltar. *Systematics and Biodiversity* 14: 394–416. <https://doi.org/10.1080/14772000.2016.1150905>
- Westerlund CA (1889) *Fauna der in der paläarktischen Region (Europa, Kaukasien, Sibirien, Turan, Persien, Kurdistan, Armenien, Mesopotamien, Kleinasien, Syrien, Arabien, Egypten, Tripolis, Tunesien, Algerien und Marocco) lebenden Binnenconchylien*. Vol. 2. Genus *Helix*. Friedländer, Berlin, 473 pp. <https://www.biodiversitylibrary.org/page/10893365>